# HYDRODYNAMICS OF AXIAL-FLOW AND CENTRIFUGAL-FLOW LEFT VENTRICULAR ASSIST DEVICES

by

James Ryan Stanfield

A dissertation submitted to the faculty of
The University of Utah
in partial fulfillment of the requirements for the degree of

Doctor of Philosophy

Department of Mechanical Engineering

The University of Utah

May 2012

## The University of Utah Graduate School

## STATEMENT OF DISSERTATION APPROVAL

The dissertation of **James Ryan Stanfield**

has been approved by the following supervisory committee members:

| | | |
|---|---|---|
| **Stacy Morris Bamberg** | , Chair | **March 6, 2012** Date Approved |
| **Eric R. Pardyjak** | , Member | **March 6, 2012** Date Approved |
| **Donald Bloswick** | , Member | **March 6, 2012** Date Approved |
| **David W. Hoeppner** | , Member | **March 6, 2012** Date Approved |
| **Craig H. Selzman** | , Member | **March 6, 2012** Date Approved |

and by **Timothy A. Ameel** , Chair of

the Department of **Mechanical Engineering**

and by Charles A. Wight, Dean of The Graduate School.

# ABSTRACT

Heart disease is the leading cause of death in the United States. Mechanical circulatory support by ventricular assist devices (VADs) is a means by which deteriorating heart function can be supplemented, and is a leading therapy for late-stage heart failure patients. The devices are commonly connected to the apex of the left ventricle (LV) to move oxygenated blood to the body via the aorta. Recent developments have made continuous-flow pumps commonplace in the clinical environment when compared to their pulsatile-flow predecessors. Typically, continuous-flow VADs are designed with axial- or centrifugal- (radial) configurations. The pressures and flow rates vary dramatically in the native heart as blood is moved from the LV to the aorta.

This dissertation presents pressure-flow characteristics for both axial- and centrifugal-flow VADs within a wide range of pressure differential values under uniform conditions, by means of a novel, open-loop flow system. Current techniques employ a closed-loop system to determine pump performance. A closed-loop system does not allow pressure differentials less than or equal to zero to be achieved. The native heart experiences pressure gradients near zero across the aortic valve during systole, which is essentially where the VAD is placed. Thus, an open-loop flow system with independently adjustable preload and afterload pressures is required to

reach physiologically-relevant pressure differential regions that approximate the pressure gradient across the aortic valve during systole.

Additional modifications made to the open-loop flow system generate pulsatile flow type conditions, which mimic those of the native LV. With this type of in vitro test system, not only can general hydrodynamic performance and hydraulic efficiency of VADs be measured, but also off-design operational performance under dynamic flow conditions can be characterized. This research explores hydrodynamic performance characteristics of axial- and centrifugal-flow VADs to determine design advantages that each have. Device characteristics include pressure-flow performance curves, pressure sensitivity, pulsatility index, and pulsatility ratio. Performance curves and other relevant attributes are investigated at previously unreported pressure-flow regions. Performance is evaluated theoretically, computationally, and experimentally under both steady-state, continuous-flow and pulsatile-flow circumstances.

CONTENTS

LIST OF FIGURES

LIST OF TABLES

# LIST OF SYMBOLS AND ABBREVIATIONS

| | |
|---|---|
| $\Delta P$ | Pressure Differential |
| $\eta_h$ | Hydraulic Efficiency |
| $\varphi$ | Flow Coefficient |
| $\psi$ | Head Coefficient |
| N | Specific Speed |
| Q | Flow Rate |
| $PI_{\Delta P}$ | Pressure Differential Pulsatility Index |
| $PI_Q$ | Flow Pulsatility Index |
| $R_e$ | Reynolds Number |
| $R_p$ | Pump Resistance |
| $R_{pul}$ | Pulsatility Ratio |
| $S_p$ | Pump Sensitivity |

| | |
|---|---|
| A1 | Axial 1 |
| A2 | Axial 2 |
| AoP | Aortic Pressure |
| AV | Aortic Valve |
| C1 | Centrifugal 1 |
| C2 | Centrifugal 2 |
| CFRBP | Continuous Flow Rotary Blood Pump |
| LA | Left Atrium |
| LV | Left Ventricle |
| LVP | Left Ventricular Pressure |
| PCC | Pulmonary Compliance Chamber |
| PI | Pulsatility Index |
| PS | Pressure Sensitivity |
| RPM | Revolutions per Minute |
| SCC | Systemic Compliance Chamber |
| VAD | Ventricular Assist Device |

# CHAPTER 1

# INTRODUCTION

This section introduces the background and motivation for the development, use and characterization of ventricular assist devices (VADs). Relevant previous work and literature is outlined. The hypotheses and contributions that form the basis for this dissertation are also presented.

## 1.1 Background

### 1.1.1 Heart Physiology

The human heart can best be described in mechanical terms as a dual-reservoir, dual-pump device. The four chambers of the heart are the right and left atria (reservoirs) and the right and left ventricles (pumps). Each ventricle has two unidirectional valves to ensure unidirectional flow in and out of the pump chamber.

Deoxygenated blood is routed through the body to the superior and inferior vena cavae, which fill the right atrium with blood. The right atrium contracts and forces the blood through the tricuspid valve and into the right ventricle. The tricuspid valve closes to prevent backflow and the right ventricle contracts. As the right ventricle contracts, the pulmonary valve opens and blood is directed to the lungs via the pulmonary artery.

Carbon dioxide and oxygen are exchanged by diffusion at the lungs and oxygen-rich blood returns to the heart via the pulmonary veins, which fill the left atrium. A similar process is repeated simultaneously on the left side of the heart. Namely, the left atrium contracts and forces the blood through the mitral valve and into the left ventricle. The mitral valve closes to prevent backflow and the left ventricle contracts. As the left ventricle contracts, the aortic valve opens and sends blood to the body via the aorta. While the right and left ventricle pump the same volume of blood during a contraction, the left ventricle generates a higher outflow pressure in order to facilitate circulation through the extremes of the entire body.

Figure 1.1 shows an illustrated cross-section of a heart. Blue arrows show the direction of flow for deoxygenated blood (to the lungs), and red arrows show the direction of flow for oxygen-rich blood (to the body).

### 1.1.2 Heart Failure

Heart disease is a leading cause of death today in the United States. The Center for Disease Control and Prevention (CDC) reports that 12% of the U.S. population has been diagnosed with heart disease. Further, the CDC's Division of Vital Statistics state that approximately 600,000 people die from diseases of the heart each year, which is about 25% of the total deaths that occur in the U.S. on an annual basis [1]. The American Heart Association (AHA) estimates that over 82 million American adults have a cardiovascular disease (CVD), and almost half of them are over 60 years of age [2].

The New York Heart Association (NYHA) has developed a classification system for levels of heart failure based on symptoms in patients such that physicians

can readily diagnose and treat the disease. Class IV is the most severe, with patients expressing symptoms at rest, and the population of this group is typically viewed as analogous to that of the CDC reported heart disease mortality rate. Class III diagnosis is for those with moderate heart disease symptoms, while Classes I and II are for functional patients with mild symptoms. The population of Class III has been estimated to be well over one million.

Various therapies exist to treat heart disease, including organ transplantation for those with the most severe cases. The U.S. Department of Health and Human Services Organ Transplantation and Procurement Network has reported an average of 2166 heart transplants occurring throughout the country each year, while the current number of patients approved and waiting for a donor heart is nearly 3200 [3].

### 1.1.3 Ventricular Assist Devices

Several heart diseases contribute to the muscular weakening of the body's pumping organ, which can reduce the flow of blood. Ventricular Assist Devices (VADs) are surgically implantable pumping devices employed to restore or support the flow of blood through the heart, and do not replace the heart organ completely [4]. VADs are implanted to either bridge a patient to transplantation (BTT) or as a long-term therapeutic alternative to transplantion, also called destination therapy (DT). It is estimated that approximately 1700 mechanical circulatory support devices are implanted each year in the U.S. as a means to aid the failing heart [5], with a potential population of over half a million, based on NYHA classification IV alone.

A Left Ventricular Assist Device (LVAD) can be surgically attached to the apex of the left ventricle and the aorta. The LVAD assists the heart by pumping blood

out of the left ventricle and into the aorta, where it is distributed to the rest of the body. VADs have been classified as first generation, second generation, and so on. First generation pumps are distinguished by volume-displacement or pulsatile-flow mechanism. Second generation pumps are continuous-flow devices with contact bearings within or near the blood flow path. And third generation devices are continuous-flow rotary pumps that employ hydrodynamic or electromagnetic suspension in place of mechanical bearings [6].

A Right Ventricular Assist Device (RVAD) is similar to an LVAD in mechanical structure and functional design, and is attached to the right ventricle of the heart to assist in pumping deoxygenated blood to the lungs. The only differences between RVADs and LVADs are the surgical placement, and the associated inflow and outflow conduits to optimize compatibility with right ventricle and pulmonary artery versus the left ventricle and aorta. In addition to conduits, smaller overall size and a lower desired operating range are distinguishing features for an RVAD compared to an LVAD as the right ventricle does not require as much pressure and flow as the left. An LVAD and an RVAD can both be connected to the heart to serve as total heart replacement [7].

VADs, like hearts, need electrical stimulation for continuous function. So while the pump itself is implanted into the body, a percutaneous cable runs from the pump to the external hardware (electrical/computer controller, power supply, etc). VADs were originally intended as short-term, bridge-to-transplant devices for patients awaiting a heart transplant. However, the devices have seen more long-term

application such as destination therapy, where they are implemented in terminally ill patients whose condition deems them disqualified for heart transplantation.

Figure 1.2 is an artistic representation of VAD placement in the circulatory system. The VAD (2) connects to the apex of the left ventricle via an inflow cannula (1), and moves blood from the ventricle chamber to the ascending aorta via an anastomosed outflow conduit (4). Also shown is the percutaneous driveline (3) by which the VAD is connected to a controller and power supply.

## 1.2 Hypotheses

Currently, continuous-flow VADs are used much more widely than those delivering pulsatile flow. While VADs have been implanted and studied for several years, an understanding of properties inherent to pump design continues to be explored under physiologic conditions. However, the current literature contains a significant deficiency of data for pressures relevant to the physiologic system, namely systolic pressure differentials that are near or equal to zero.

The objective of this research is to explore VAD performance characteristics at physiologically-relevant conditions, but specifically including systolic pressure differentials near or equal to zero.

It is hypothesized that centrifugal-flow VADs are more optimal, in a physiologically compatible sense, than axial-flow pumps. Centrifugal-flow devices exhibit flow properties more conducive to native heart function. Performance characteristics include pressure-flow performance curves, pressure sensitivity, pulsatility index and pulsatility ratio.

To address the objective of this research and characterize VAD performance at physiologically-relevant conditions, including systolic pressure differentials near zero, the following scientific questions will be investigated:

1. Evaluate how flow characteristics of axial- and centrifugal-flow VADs compare to one another and to the native heart, by:
    a. Investigating the shape of performance curves at previously unreported pressure-flow regions.
    b. Understanding what the shape of performance curves at previously unreported pressure-flow regions indicate.
    c. Evaluating how the shape of performance curves at previously unreported pressure-flow regions similar to previously assumed data.
2. Evalutate how device performance (pressure sensitivity) of axial- and centrifugal-flow VADs compare to one another under theoretical physiological conditions.
3. Evaluate how device performance (pulsatility index, etc.) of axial- and centrifugal-flow VADs compare to one another under experimental *in vitro* conditions.

It is hypothesized that continuous-flow VADs with centrifugal design will have higher hydraulic efficiency, be more pressure-sensitive, and have higher pulsatility than those of axial-flow design. Particulars for each of the three hypotheses are presented with detailed methods, results, discussions, and conclusions in Chapters 2, 3, and 4, respectively, in this dissertation. The basis for the three hypotheses is a combination of design theory, anecdotal experience, and intuition.

## 1.3 Contributions

This research addresses a knowledge gap in the analysis of ventricular assist devices (VADs) at physiologically-relevant conditions. Namely, but not limited to, the performance characteristics of VADs operating during systole (low transaortic pressure gradient). It will be shown that pressure-flow performance data can be determined for any VAD by means of the novel application of an open-loop flow system. This project will afford surgeons an increased knowledge and understanding of VAD operation relevant to physiologic performance, aid in patient-education for device selection, and improve diagnosis of implanted patients. This project will show engineers and clinicians alike the differences in performance between axial- and centrifugal-flow devices. Performance will be evaluated theoretically, computationally, and experimentally under both steady-state, continuous flow and pulsatile flow circumstances.

## 1.4 References

1. Kochaneck KD, Xu J, Murphy SL, Minino AM, Kung HC. Deaths: Preliminary data for 2009. National Vital Statistics Reports 2011.

2. Roger VL, Go AS, Lloyd-Jones DM, et al. AHA statistical update: Heart disease and stroke statistics–2012 update: A report from the American Heart Association. Circulation 2011.

3. Organ Procurement and Transplantation Network. United States Department of Health and Human Services, 2011. http://optn.transplant.hrsa.gov

4. Kormos RL, Miller LW. Mechanical Circulatory Support: A Companion to Braunwald's Heart Disease. Amsterdam: Elsevier; 2011.

5. Birks EJ. The comparative use of VADs: Differences between Europe and the United States. Tex Heart Inst J 2010; 37:565-567.

6. Olsen DB. The history of continuous-flow blood pumps. Artificial Organs 2000; 24:401-404.

7. Frazier OH, Tuzun E, Cohn W, Tamez D, Kadipasaoglu KA. Total heart replacement with dual centrifugal VADs. ASAIO Journal 2005, 51:224-229.

8. National Heart Lung and Blood Institute, National Institutes of Health. How the heart works: Anatomy of the heart. United States Department of Health and Human Services, 2011. http://www.nhlbi.nih.gov/health/health-topics/images/heart_interior2011.jpg

9. Thoratec HeartMate II LVAS. Reprinted with permission from Thoratec Corporation.

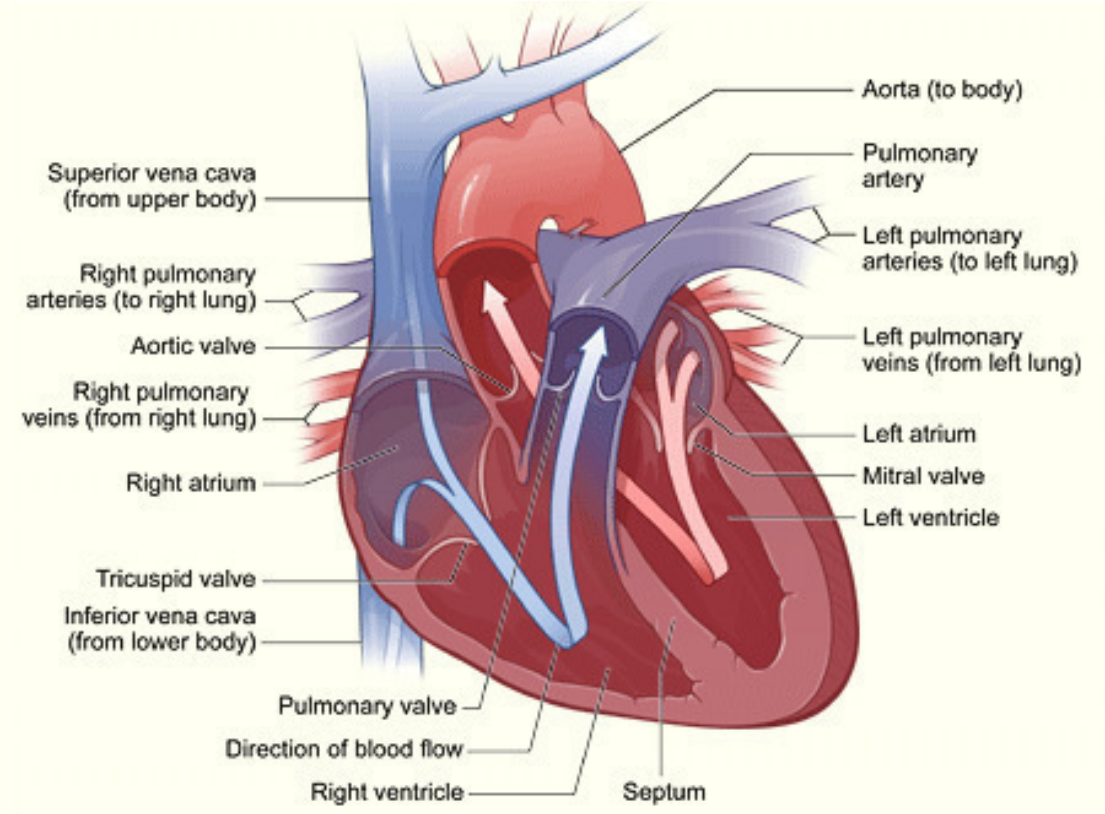


Figure 1.1. Heart interior [8]. Courtesy NHLBI, NIH, DHHS.

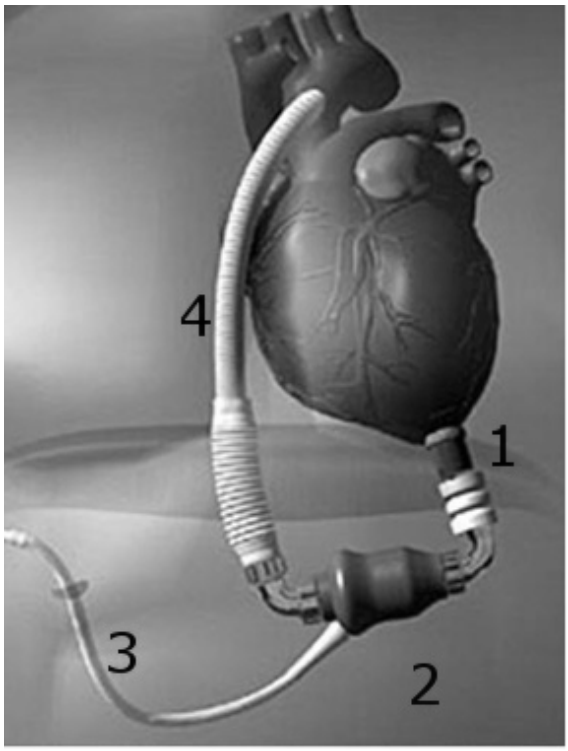


Figure 1.2. Device connection to the native heart [9]. Connection of the device inflow port to the left ventricular apex (1); Pump (2); Percutaneous driveline cable (3); Outflow graft anastomosed to ascending aorta (4).

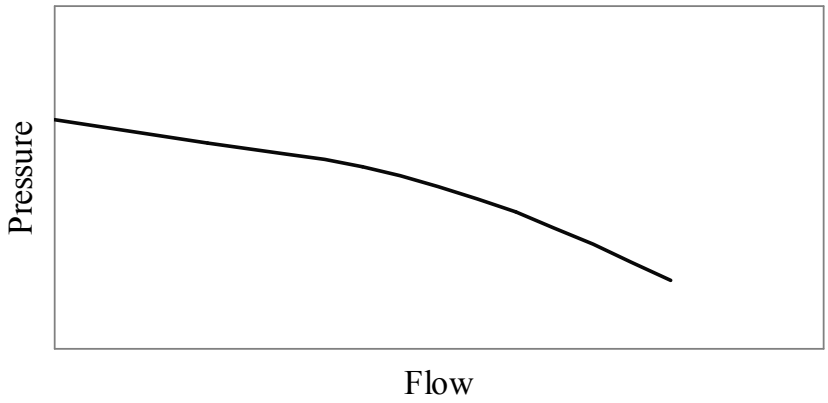


Figure 1.3. Generic pressure-flow performance curve.

# CHAPTER 2

# FLOW CHARACTERISTICS OF AXIAL-FLOW AND CENTRIFUGAL-FLOW LEFT VENTRICULAR ASSIST DEVICES

Fluid pumping technology has been around for centuries, and is well understood and documented. However, the pump design optimization techniques accepted in industry are geared toward steady-state constant flow conditions. In contrast, the implantation of a continuous flow pump to aid the output of the human left ventricle subjects the device to perpetual variation. This study measures pressure-flow performance characteristics for both axial- and centrifugal-continuous flow rotary blood pumps across a wide range of pressure differential values under uniform conditions by means of a novel open-loop flow system. The axial-flow devices show greater hydraulic losses and lower hydraulic efficiency. All pumps yield greatest hydraulic efficiency at a head to flow coefficient ratio of approximately 1.7. The open-loop flow system accounts for the dynamic changes associated with human heart physiology and allows for more precise characterization of existing heart pumps, as well as those in development.

## 2.1 Introduction

Typical design practices for rotodynamic fluid pump configurations, axial or centrifugal, are centralized around a specific speed for a desired pressure and flow [1,2]. Classically, axial-flow pumps tend to be used under high flow rate and low head pressure conditions, while centrifugal-flow pumps are designed for lower flow rate and higher head conditions. Many rotodynamic pumps used around the world are employed under stable fluid pressure conditions that do not exhibit continuous variation. Unfortunately, this is not the case with ventricular assist devices (VADs) placed within the dynamic environment of the human heart. VADs are exposed to broad ranges of preload, or left ventricular pressure (LVP), and afterload, or aortic pressure (AoP), when implanted in the circulatory system. Typical blood pressures are 120/80 (mmHg; systolic/diastolic), and flows are 5.5 L/min for healthy adults [3]. While in this configuration the transaortic pressure gradient (AoP – LVP) can have an impact on the output of the device [4]. The transaortic pressure gradient is greatest during end-systole and early diastole, where high arterial and decreasing ventricular pressures exist, and approaches zero during systole when the aortic valve is open. Thus, the application of typical pump design parameters for ideal performance over the range of physiological pressures is not viable [5].

Many reports have been published on the performance characteristics of individual VADs [6-8]. Reports available in the published literature employ a closed-loop hydraulic circuit to characterize device performance (Figure 2.1a), where pressures may be measured near the inlet and outlet of the pump, outflow is measured, and outflow pressure may be varied by a valve or other similar means. However, due

to the physical, hydrodynamic limitations of the closed-loop systems that are employed for device characterization, only a limited range of flow rate (Q) and pressure differential (ΔP) values are reported [9]. The closed-loop hydraulic system is an acceptable tool used to collect a limited amount of data; however, because the outflow is directly connected to the inflow, ΔP down to a certain minimal threshold may be achieved and nothing lower. As such, current devices utilizing this system are not actually tested over the full range of physiologically-relevant pressure-flow conditions.

The study of flow characteristics of rotodynamic pumps can yield a wealth of information. Yet, few reports test and analyze multiple devices under the same conditions (system, resistances, fluid temperature, fluid viscosity, etc) [10]. No reports compare performance characteristics and design constants of both axial- and centrifugal-flow VADs to one another. Functionality of axial- and centrifugal-flow devices can be compared to one another by examination of the performance curves and dimensionless analysis of impeller speed, fluid pressure and fluid flow. Dimensional analysis of device performance will yield details on specific speed and general performance, which further show the hydraulic losses and efficiency of each device. As a consequence, performance can be compared between multiple devices.

In this study, pressure-flow characteristics for both axial- and centrifugal-flow VADs are measured over a wide range of uniform physiologically-relevant conditions, by means of a novel, open-loop flow system.

## 2.2 Methods

A novel mock circulatory loop (Figure 2.1b) was designed to measure pump preload, afterload, and output flow rate under different operating conditions. The loop consisted of an acrylic 20-L reservoir with weir filled with a blood-analog fluid (~40% glycerin in water at 36 °C; Hi-Valley Chemical, Centerville, UT) that had a dynamic viscosity of 3.6 cP, and a density of 1.13 g/cc. The adjustable weir was used to maintain a steady inflow pressure to the LVAD, which was connected to both upper and lower reservoirs by Tygon® tubing (Saint-Gobain, Courbevoie, France). A manual gate valve was placed in series with the LVAD to adjust the resistance (afterload). Four continuous flow rotary blood pumps were tested, two axial-flow, and two centrifugal-flow.

Pump preload, or inflow pressure ($P_i$), and pump afterload, or outflow pressure ($P_o$) were measured with fluid-filled transducers (Edwards LifeSciences, Irvine, CA), and a pressure meter (Living Systems Instrumentation, St. Albans, VT). The pump flow rate (Q) was measured with an ultrasonic flow meter and flow probe (Transonic, Ithaca, NY). Acquisition of flow meter and pressure meter data signals was performed at 40 Hz with a custom system (National Instruments, Austin, TX), and output to a comma separated values (csv) file.

The four devices analyzed will be referred to hereafter as Axial 1 (A1), Axial 2 (A2), Centrifugal 1 (C1) and Centrifugal 2 (C2). A1 was operated between 7000 and 13000 rpm at 200-rpm increments. A2 was operated between 8000 and 12000 rpm in 1000-rpm increments. C1 was operated between 800 and 3000 rpm, and C2 was operated between 1800 and 3000 rpm, both at 200-rpm increments. The resistance was

varied from minimal to maximal with the manual gate valve at each pump speed. Flow rate was allowed to stabilize in 0.25 L/min increments. Pressure differential across the pump ($\Delta P = P_o - P_i$) was recorded manually in increments of 1 L/min to ensure the integrity of the data acquisition (DAQ) system.

For data analysis and plotting, MATLAB (v6.5; MathWorks, Natick, MA) and a spreadsheet program (Excel 2007, Microsoft, Redmond, WA) were used. The relationship between pump flow rate and differential pressure was extracted from the original 40 Hz csv files and tabulated in another spreadsheet file at 0.25-L/min increments for all applicable speeds.

## 2.3 Calculations

Dimensionless quantities for pump flow or the so-called pump affinity laws have been well established for fluid dynamic analysis and comparison of pumps [1]. The analysis here includes nondimensional performance parameters such as specific speed ($N$), head coefficient ($\psi$), flow coefficient ($\varphi$), Reynolds number ($R_e$) and hydraulic efficiency ($\eta_h$). Specific speed is calculated by equation 2.1, where $\Omega$ is rotational speed of the impeller [rad/s], $Q$ is flow [$m^3/s$], $H$ is head [Pa], and $g$ is acceleration due to gravity [$m/s^2$]. Employing consistent metric units will yield a dimensionless $N$.

$$N = \frac{\Omega Q^{1/2}}{(gH)^{3/4}} \tag{2.1}$$

$$\psi = \frac{gH}{R^2\Omega^2} \tag{2.2}$$

$$\varphi = \frac{Q}{AR\Omega} \tag{2.3}$$

Performance curves for any given impeller speed are unified into a single curve via the nondimensionalization of pressure (or head) and flow. Equations 2.2-2.3 are used to gauge characteristic coefficients for head ($\psi$) and flow ($\varphi$), where $R$ is the radius of impeller [m], and $A$ is the area of inlet or outlet [$m^2$]. Reynolds number and hydraulic efficiency are defined by equations 2.4-2.5.

$$R_e = \frac{2\rho\Omega R^2}{\mu} \tag{2.4}$$

$$\eta_h = \frac{Q\Delta P}{T\Omega} \tag{2.5}$$

where $\rho$ is the fluid density, $\mu$ is dynamic viscosity, and $T$ is the torque applied by the impeller to the fluid.

Another point of interest for pump designers is the pump resistance ($R_p$), which is commonly defined by the slope of the performance curve. Equation 2.6 characterizes the pump resistance function in nondimensional terms. Finally (equation 2.7), pump sensitivity ($S_p$), is hereby described as the inverse of pump resistance.

$$R_p = -\frac{d\psi}{d\varphi} \tag{2.6}$$

$$S_p = -\frac{d\varphi}{d\psi} \tag{2.7}$$

## 2.4 Results

Utilizing our open loop configuration, pressure-flow performance curves were generated for each LVAD (Figure 2.2). ΔP values down to zero were obtained for all devices. The range of data for ΔP = 0 is crucial because the physiological system (AoP – LVP) can reach this region during systole [4]. Q continues to increase as ΔP decreases, for all values that were measured here. The performance curves for axial- and centrifugal-flow pumps are relatively typical in that the pressure for centrifugal-flow pumps is reasonably flat and the pressure gradually decreases as flow increases, and the curves for axial-flow are much steeper and comparatively linear [2]. With the pressure-flow data taken on the continuous-flow mock loop, shown here, theoretical pump design parameters are analyzed and compared.

The Reynolds number, a dimensionless ratio of inertial to viscous forces, has been defined by equation 2.4, and while similar to the form for uniform flow within a pipe does not have the same connotation associated with laminar or turbulent flows. Reynolds numbers associated with pumps have more to do with pump size, cavitation, and thus, hydraulic efficiency [11]. Evaluation of Reynolds number under typical operational ranges is significant because it establishes a metric for drag at a device-fluid interface. Table 2.1 contains the Reynolds number values over which each device was operated. Further, hydraulic efficiencies (equation 2.5) for each device at operational $R_e$ are plotted against flow coefficient in Figure 2.3. Of the four, C2 achieves the highest $\eta_h$ over the broadest range of $\varphi$, and A2 reaches the lowest peak $\eta_h$ this time over the smallest range of $\varphi$.

Performance curves for any given impeller speed are unified into a single curve via the dimensional analysis for head and flow coefficients. The nondimensional performance curves for each device are shown in Figure 2.4a. The A1 and C1 devices show corresponding head versus flow properties, especially for the $0.5 < \varphi < 1.5$ regime. The other two curves imply greater and fewer hydraulic losses for the A2 and C2 pumps, respectively. Maximum $\psi$ values, where $\varphi = 0$, are .45, .29, .37 and .57 for A1, A2, C1 and C2, respectively. Similarly, maximum $\varphi$ values, where $\psi = 0$, are .22, .13, .20 and .50 for A1, A2, C1 and C2, respectively.

The hydraulic efficiency of a pump is the ability to conduct fluid with minimal loss. Understanding of hydraulic energy losses, or efficiency, is key to evaluating the global design of the fluid flow path. Hydraulic efficiency is not to be confused with overall system efficiency. For example, VAD systems require power supplies and controllers. Each system controller is designed separately, and therefore has a unique way of operating the pump. Pump impellers are connected to motors that induce rotation. The efficiencies of the motors and controllers contribute to the overall system efficiency, but are separate from the hydraulic efficiency.

The maximum hydraulic efficiency occurs at the same $N$, $\psi$ and $\varphi$, regardless of Reynolds number, or impeller speed. The values of the nondimensional parameters for each device at peak efficiency are also presented in Table 2.1. $\psi$ and $\varphi$ points at peak $\eta_h$ are plotted graphically along with nondimensional performance curves in Figure 2.4a, while Figure 2.4b displays the pressure-flow regimes represented by the most efficient specific speeds for each pump. Specific speed for a pump impeller is used to show pump characteristics over a range of pressure and flow values. During

design, specific speed is implemented to define physical properties and flow types for pumps. It is most intriguing to note that all four devices experience maximum $\eta_h$ at nearly the same point where the $\psi/\varphi$ ratio is approximately 1.7. While the $\psi/\varphi$ ratio is similar for all four devices at peak $\eta_h$, the optimal operating flow regime for the A2 device, is markedly different than that observed for the other three pumps.

Continual analysis of the dimensionless values from the pressure-flow performance curves can yield further insight to a pump's functionality. Pump resistance is usually a positive value for design flow conditions, but can be negative at low flow rates [2]. An additional quantity, pump sensitivity, can be related from $\psi$, $\varphi$ and $R_p$. High sensitivity values indicate that a pump will have a large change in output for a small change in pressure (equations 2.6-2.7).

Pump sensitivity and pump resistance are important quantities that provide an understanding of how a device will behave under fluctuating operating conditions. Quantification of the details may produce a metric related to hemo- and/or bio-compatibility. Figure 2.5 presents $R_p$ and $S_p$ as a function of $\varphi$ and as a function of $\psi$ for each of the evaluated devices. While the resistance and sensitivity functions for each pump vary, a general observation can be made that the continuous flow pumps show increasing resistance with increasing flow and decreasing head, and conversely, increasing sensitivity with increasing head and decreasing flow. Minimum resistance and maximum sensitivity for both A2 and C1 occur where $\varphi = 0$, and correspondently, maximum resistance and minimum sensitivity for both occur where $\psi = 0$. The other two devices exhibit similar behavior in general; however, upon closer inspection local minima and maxima can be found on the dimensionless functions of resistance and

sensitivity. Minimum resistance and maximum sensitivity occur at ($\psi$, $\varphi$) = (.28, .11) and (.56, .08) for A1 and C2, respectively. Whereas, the maximum resistance and minimum sensitivity are found at (.04, .21) and (.10, .38), respectively.

## 2.5 Discussion

The effects and implications of our open-loop mock flow system are discussed herein. Theoretical pump design parameters using the pressure-flow data are analyzed and compared. Similarities between axial- and centrifugal-flow device hydraulic performance, as well as pump resistance and pump sensitivity are explored.

As displayed in Figure 2.2, our open-loop mock flow system effectively achieves extensive pressure-flow regimes across both axial- and centrifugal-flow implantable blood pumps, demonstrating the effectiveness and benefit of using a slightly more complex system for hydraulic analysis. The open-loop flow system is capable of achieving $\Delta P$ values that are scientifically-relevant for a device that will be placed in parallel with the physiologic system. It is recommended that future analyses of such devices be done under conditions that resemble the open-loop flow system.

Nondimensionalization of flow characteristics, by removing units that involve physical measures, can simplify and scale the hydrodynamic system. Additionally, further information regarding the performance properties of a system can be revealed. The dimensionless values outlined previously are common practice in fluid flow analyses. For example, the nondimensionalization of pressure-flow performance curves taken over several rotational speeds for a given rotodynamic pump will yield a single performance curve. From the dimensionless performance curve general

observations can be made regarding hydraulic losses that the device is subject to, and thus, hydraulic efficiency can be inferred.

Several conditions can contribute to hydraulic loss, including friction at the fluid-pump interface, pump size, surface area and geometry, cavitation, turbulent flow, and more. The ideal, lossless pump will exhibit a straight line for the $\psi$–$\varphi$ curve. However, in reality all pumps are subject to hydraulic losses, and thus, will be somewhere below the ideal $\psi$–$\varphi$ line. Consequently, the further a dimensionless performance curve lays below the ideal straight line, the stronger the implication that the pump has higher hydraulic losses.

Specific speed for a pump impeller is used to show pump characteristics over a range of pressure and flow values. During design, specific speed is implemented to define physical properties and types for pumps. An increase in pump size is said to increase the operating Reynolds number, and increase the hydraulic efficiency.[11] The hydraulic efficiency of a pump is the ability to conduct fluid with minimal loss. Understanding of hydraulic energy losses, or efficiency, is key to evaluating the global design of the fluid flow path. Hydraulic efficiency is not to be confused with overall system efficiency. For example, VAD systems require power supplies and controllers. Each system controller is designed separately, and as such has a unique way of operating the pump. Pump impellers are connected to motors that induce rotation. The efficiencies of the motors and controllers contribute to the overall system efficiency, but are separate from the hydraulic efficiency.

Physically speaking, the centrifugal-flow pumps employed here are not significantly greater in overall size than those designed for axial-flow, but Figure 2.4a

shows that they have greater capacity for pressure and flow. The average centrifugal and axial curves deduced from this figure demonstrate that the centrifugal curve would have greater ($\psi$,$\varphi$) values than that of the axial. This suggests that the centrifugal-flow pumps have fewer hydraulic losses, and thus greater hydraulic efficiency. However, the A1 and C1 devices yield similar dimensionless flow characteristics and hydraulic efficiency. The dimensionless performance curves for the A2 and C2 pumps are below and above, respectively, the region where A1 and C1 reside. An interesting finding is illustrated by comparing Figures 2.3 and 2.4 where hydraulic efficiencies for each pump are roughly correlated with the location of dimensionless performance curves.

The internal flow-path volumes of both axial-flow pumps are relatively similar. The flow-path volumes of C1 and C2 devices are two and three times greater than the axial pumps, respectively. Hydraulic efficiency may be related to pump size, but this is not always readily apparent. In these results, a correlation between hydraulic efficiency and pump size is seen only when comparing axial-to-axial or centrifugal-to-centrifugal. No association is observed when comparing axial-flow and centrifugal-flow volume or size to efficiency or performance. This confirms the notion that several factors impact the efficiency of fluid flow, including pump size, blade geometry, surface area, maximum and minimum gap size, and more.

A similar $\psi/\varphi$ ratio for all four devices at peak efficiency is of great significance, and almost compels a conclusion that all pumps were independently designed to the same specification. However, upon examination of the operational range of the hydraulically efficient specific speeds, or design-specific speeds, it is noticeable that one of the axial-flow devices (A2) operates most efficiently in a

pressure-flow regime considerably apart from the other three devices. This shows that at least one of the devices was designed for a slightly different functional environment. However, it is worthy to note that hydraulic efficiency is not nor should it be the primary concern when designing a continuous flow blood pump. The primary objective for these devices is to move blood without causing hemolysis or thrombosis to the working fluid, so compromises in the fluid flow path are to be expected when dealing with a long term life support device.

Generally, the continuous flow pumps show increased resistance with high $\varphi$ and low $\psi$, and conversely, increased sensitivity with high $\psi$ and low $\varphi$. Of particular interest is that C1 and C2 reveal much lower resistance, possibly due to the centrifugal flow path itself, than that within the realm of capability for A1 and A2. Assuming the human cardiovascular system is more compatible with flows corresponding to low $\varphi$, it would then behoove one to opt for a device with low resistance and high sensitivity. This being the case, the centrifugal-flow path may be the best suited for physiologic implantation.

The resulting analyses presented here position dimensionless values and equations as the center of attention. Particular interest has been given to hydraulic efficiency of axial- versus centrifugal-flow devices. Head and flow coefficients, pump resistance and pump sensitivity have all been explored. However, our results should be interpreted with several caveats.

First, the flow characteristics and physiological similarities for a mechanical pump, axial or centrifugal, when connected in parallel with a pulsating pump, such as the device configuration when implanted, is not evaluated here. Evaluation of pump

performance under pulsating preload and afterload conditions, could be highly beneficial when comparing devices to one another and to the native heart, and is recommended for future work. Second, this study examines the flow characteristics of different VADs under continuous flow conditions. Standard design practices for fluid-pumping systems have been set up for constant flow relationships, and do not consider pulsatile conditions [1,2]. The difference in peak efficiency flow regimes between devices can be explained by the need to operate the device under a wide range of preloads and afterloads because the intended use in parallel with a human heart is not only for an individual human system, but also across a diverse array of the potential human population. Finally, hemocompatibility assessment of the devices is not carried out here. Damage to cellular structures within the transported fluid is another concern that VAD design should consider and the tradeoffs that it may impart to hydraulic efficiency. Only global performance of each device is assessed without consideration of local phenomenon such as backflow, turbulence, flow path design, surge, auto-oscillation, etc.

## 2.6 Conclusions

The open-loop flow system was successfully able to generate $\Delta P$ across the pumps at levels equal to or less than zero, thus making a more clinically-relevant assessment of pump function. A dimensionless assessment of the flow characteristics yields favorable results for the average of the centrifugal-flow devices as they demonstrate greater capacity, fewer hydraulic losses, and thus, greater hydraulic efficiency when compared to the axial-flow devices. The benefit of hydraulic efficiency may be associated with physical size or priming volume. Further, the

centrifugal-flow VADs demonstrate lower resistance, which implies greater sensitivity, than the axial-flow designs for low values of flow. Thus, from a purely hydraulic analysis point of view, we propose the centrifugal-flow pumps to be more effective than axial-flow devices.

## 2.7 References


1. Stepanoff AJ. Centrifugal and Axial Flow Pumps: Theory, Design, and Application. Wiley; 1948.

2. Brennen CE. Hydrodynamics of Pumps. Cambridge; 2011.

3. Berne RM, Levy MN. Cardiovascular Physiology, 8th ed. Mosby; 2001.

4. Saxton GA Jr, Andrews CB. An ideal heart pump with hydrodynamic characteristics analogous to the mammalian heart. ASAIO Trans 1960; 6:288-291.

5. Wu ZJ, Antaki JF, Burgreen GW, Butler KC, Thomas DC, Griffith BP. Fluid dynamic characterization of operating conditions for continuous flow blood pumps. ASAIO J 1999; 45:442-449.

6. Griffith BP, Kormos RL, Borovetz HS, et al. HeartMate II LVAS: from concept to first clinical use. Ann Thorac Surg 2001; 71:S116-20.

7. Frazier OH, Myers TJ, Jarvik RK, et al. Research and development of an implantable axial-flow LVAD: the Jarvik 2000 Heart. Ann Thorac Surg 2001; 71:S125-32.

8. Tansley G, Vidakovic S, Reizes J. Fluid dynamic characteristics of the VentrAssist rotary blood pump. Artif Organs 2000; 24:483-87.

9. Farrar DJ, Bourque K, Dague CP, Cotter CJ, Poirier VL. Design features, developmental status and experimental results with the Heartmate III centrifugal LVAS with magnetically levitated rotor. ASAIO J 2007; 53:310-15.

10. Frazier OH, Khalil HA, Benkowski RJ, Cohn WE. Optimization of axial-pump pressure sensitivity for a continuous-flow TAH. J Heart Lung Transplant 2010; 29:687-91.

11. Karassik IJ, Messina JP, Cooper P, et al. Pump Handbook, 2nd ed. McGraw-Hill; 1986.

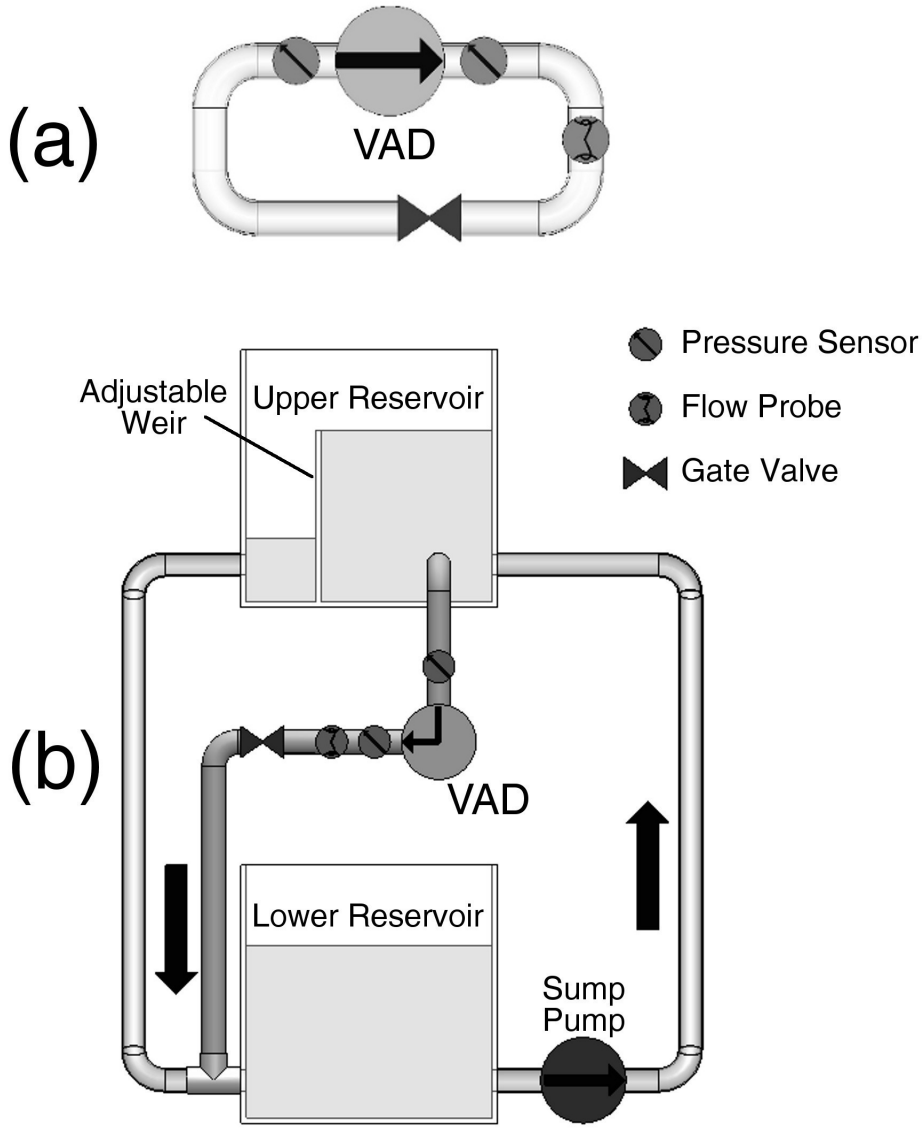


Figure 2.1. Typical closed-loop flow system (a). Open-loop flow system designed to impose low and high extremes of pressure differential on tested ventricular assist devices (b).

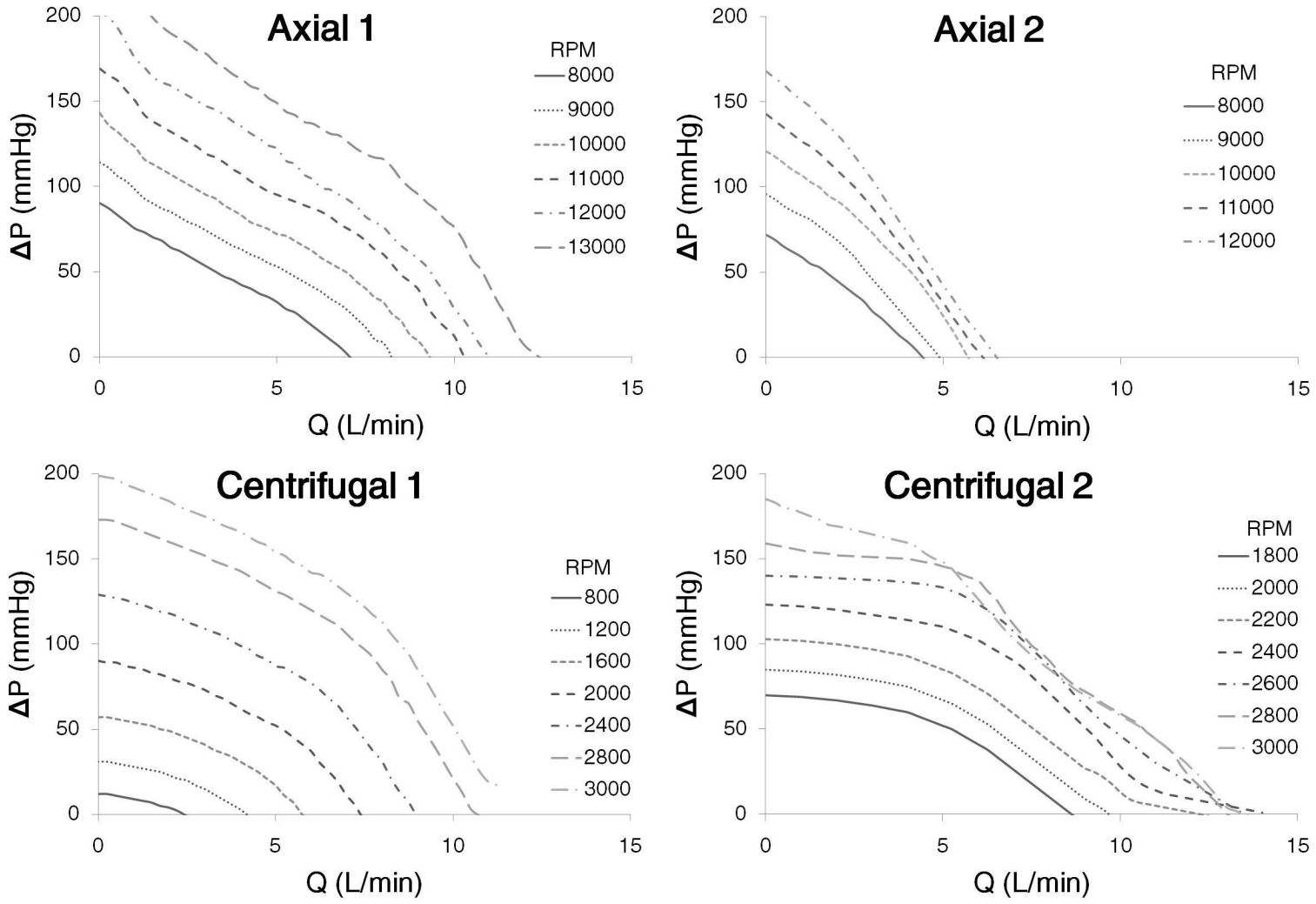


Figure 2.2. Characteristic pressure-flow curves for each VAD. *ΔP*, pressure differential; *Q*, pump flow rate.

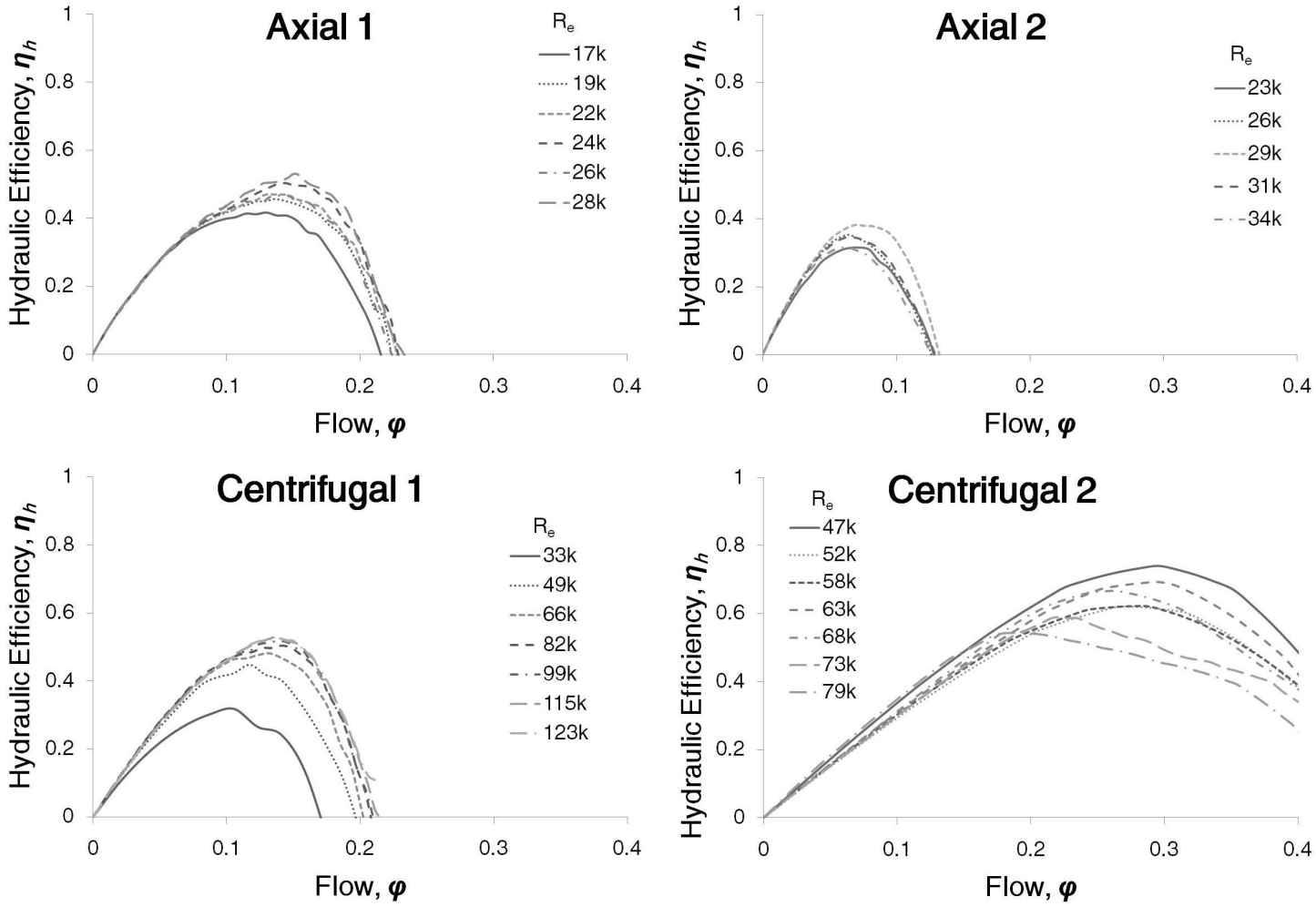


Figure 2.3. Hydraulic efficiencies for each device at each operational Reynolds number with respect to flow. $\varphi$, flow coefficient; $\eta_h$, hydraulic efficiency.

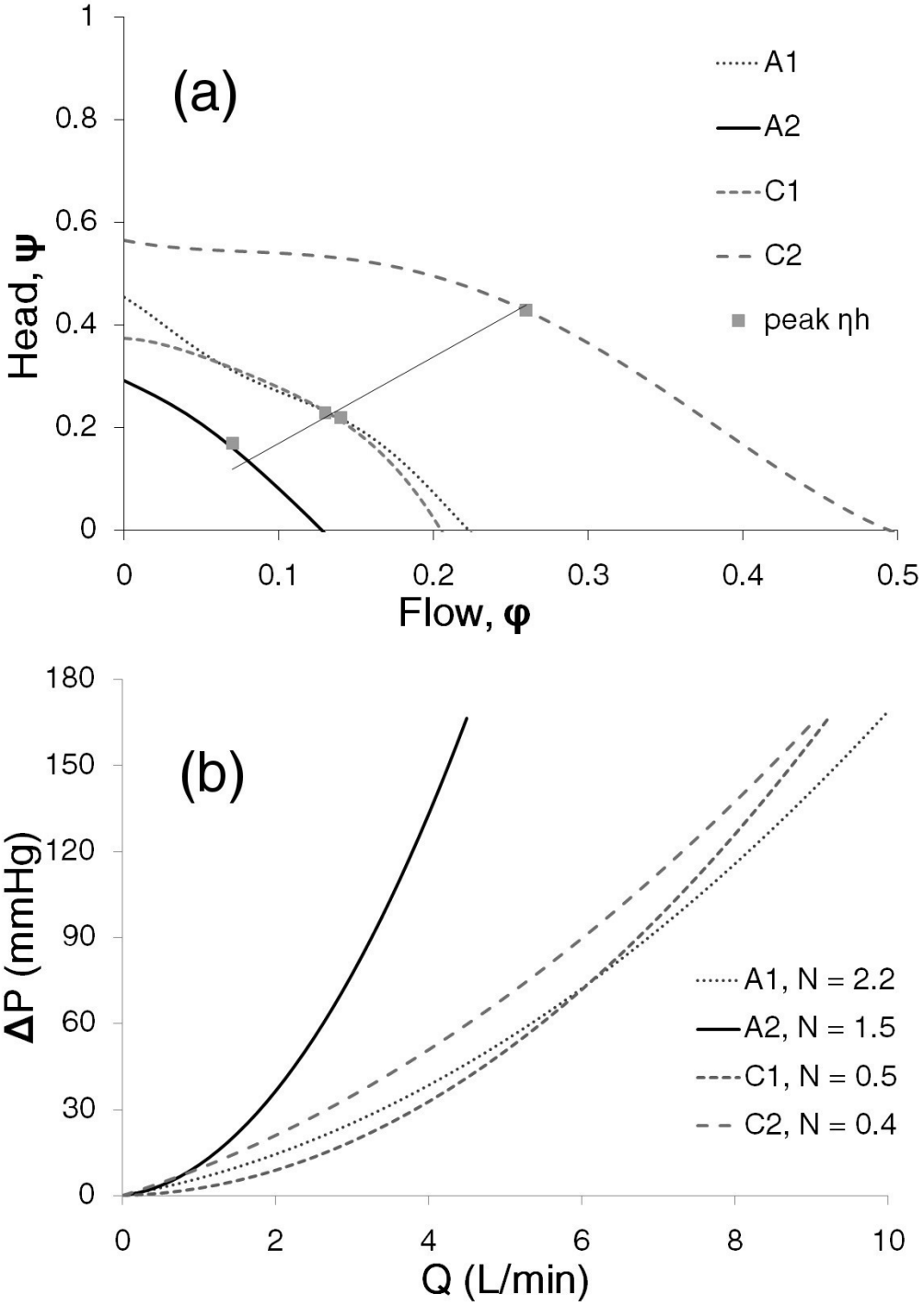


Figure 2.4. Dimensionless performance curves for each ventricular assist device marked with points of peak hydraulic efficiency (a). Peak hydraulic efficiency specific speeds displayed against flow regime (b). $\psi$, head coefficient; $\varphi$, flow coefficient; $\eta_h$, hydraulic efficiency; $\Delta P$, pressure differential; $Q$, pump flow rate; $N$, specific speed.

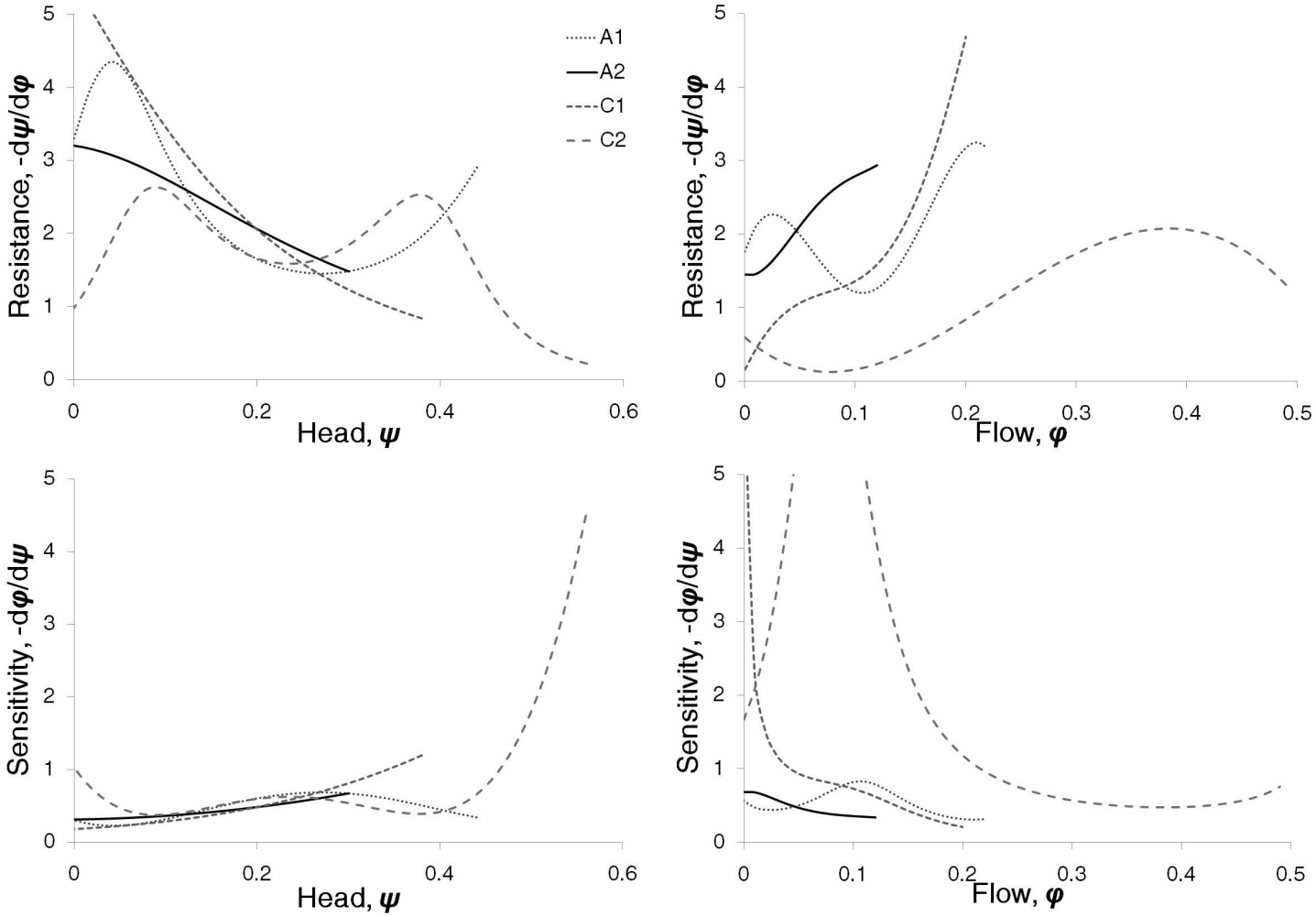


Figure 2.5. Pump resistance and sensitivity as a function of flow and as a function of head for each ventricular assist device. $\psi$, head coefficient; $\varphi$, flow coefficient; $R_p$, pump resistance; $S_p$, pump sensitivity.

Table 2.1. Reynolds number ranges for all recorded operational speeds for each device and calculated nondimensional parameters for each device at peak efficiency over entire operational range. $R_e$, Reynolds number; $N$, specific speed; $\psi$, head coefficient; $\varphi$, flow coefficient.

| | **Axial 1 (A1)** | **Axial 2 (A2)** | **Centrifugal 1 (C1)** | **Centrifugal 2 (C2)** |
|---|---|---|---|---|
| $R_e$ range (x1000) | 17-28 | 23-34 | 33-123 | 47-79 |
| $N$ | 2.2 | 1.5 | 0.5 | 0.4 |
| $\psi$ | .22 | .17 | .23 | .43 |
| $\varphi$ | .14 | .07 | .13 | .26 |

# CHAPTER 3

# PRESSURE SENSITIVITY OF AXIAL-FLOW AND CENTRIFUGAL-FLOW LEFT VENTRICULAR ASSIST DEVICES

Continuous-flow ventricular assist devices (CF-VADs) defy normal physiologic principles associated with pulsatile flow. Despite being programmed at set speeds, pump flow can be modified by variations in the pressure differential across the pump, termed pressure sensitivity (PS). Currently, PS has been reported using closed-loop systems that are unable to provide physiologically-relevant assessment of PS or account for partially- or fully-unloaded ventricles. We report a unique model system to examine PS and its influence on efficiency of CF-VADs.

A mock-circulation loop was designed that measures low and high extremes of pressure differential. Two axial-flow and two centrifugal-flow VADs were tested. Device output flow rate, preload, and afterload were measured and PS was calculated. Analytical models were implemented to study "fully-loaded," "partially-unloaded," and "fully-unloaded" cardiac cycles.

Our open-loop model successfully generated physiologically-relevant pressure gradients across the pump. All devices exhibit highest PS during early diastole; however, average PS values of centrifugal-flow were 4x greater than axial-flow

devices. At clinically-relevant speeds under fully-unloaded conditions, where ventricular pressure never reaches the aortic pressure, average flow rate decreased by 41%. The average maximum PS for the axial and centrifugal VADs under physiologic conditions was 0.08 and 0.30 L/min/mmHg, respectively.

Compared to axial-flow pumps, centrifugal-flow VADs demonstrate increased PS at intermediate to low flow rates. Enhanced device PS allows for more effective self-regulation of device output, thus allowing a given VAD to better mimic the native heart under exercise conditions, and minimize undesirable effects, including ventricular suck-down or atrial collapse.

## 3.1 Introduction

During the cardiac cycle, the left ventricle undergoes large changes in pressure [LVP] compared to those experienced in the ascending aorta [AoP]. As the ventricle contracts during early systole, LVP increases prior to opening of the aortic valve (AV), followed by an equilibrated transaortic pressure gradient while the AV is open and subsequent ejection of blood from the LV to the ascending aorta [1]. This normal pattern of generating cardiac output in the cardiac cycle is significantly altered in patients with left ventricular assist devices (LVADs). In the earlier era of VADs, pulsatile devices essentially replaced myocardial function by working in series with the heart, thus bypassing the functional cardiac cycle [2-4]. The increasing use of continuous flow blood pumps has changed the way we approach patients with these devices by working in parallel with native heart function. Thus, effective cardiac output is dependent upon optimizing both device and native cardiovascular function.

The transaortic pressure gradient (AoP – LVP) is greatest during end-systole and early diastole, where high arterial and decreasing ventricular pressures exist, and approaches zero during systole when the aortic valve is open. With continuous-flow pumps, the transaortic pressure gradient can have a significant impact on the output of the device [5]. Although not pulsatile by design, these pumps are sensitive to preload and afterload pressure variations [6]. At a constant impeller speed, the output flow rate (Q) of a VAD can change dramatically depending on the pressure differential (ΔP) across the pump [7]. A device that is highly pressure sensitive will have a large change in Q for a small change in ΔP. Thus, pressure sensitivity (PS) is the rate of change of flow with respect to the rate of change of pressure. Computationally, this equates to the slope of the characteristic pressure-flow curve, or the first-derivative of flow with respect to pressure, which can be defined as $dQ/d\Delta P$. PS measurement is important because it signifies how responsive a device will be under certain operating conditions.

Several studies have been undertaken to evaluate the PS of various VADs [8,9]. Few reports have been found where multiple devices are tested and analyzed under the same conditions [10]. Furthermore, pressure-flow characteristics for VADs are reported for a limited range of Q and ΔP values [11]. Finally, no reports exist that compute the theoretical Q and PS for a partially- or fully-unloaded ventricle.

The lack of available data is related to device testing within a closed -loop system. A closed-loop mock circulatory flow system will not be able to simulate low or negative ΔP or negative flow due to physical, hydrodynamic limitations. Low ΔP has significant clinical and physiological importance because that is what is experienced by the mammalian circulatory system during systole. A closed-loop flow

system is one where the preload is dependent upon the generated afterload because they are directly connected, so preload or afterload cannot be adjusted without affecting the other. Therefore, all existing *in vitro* data with regards to continuous flow VADs are based on nonphysiologic modeling.

Conversely, an open-loop system is free from dependency restrictions such that both preload and afterload are independently adjustable. During the systolic portion of the cardiac cycle the pressure differential between the ascending aorta and LV approaches zero, which is why measurement of flow characteristics at low or negative $\Delta P$ is clinically significant. While systole is just fractions of a second, it still comprises approximately one-third of the cardiac cycle. As such, we sought to examine pressure-flow characteristics for both axial- and centrifugal-flow VADs within a wide range of $\Delta P$ values under uniform conditions, by means of a novel, open-loop flow system.

## 3.2 Methods

We analyzed four VADs, two with axial-flow design and two with centrifugal-flow (or radial-flow) design. From here, the devices will be referred to as Axial 1 (A1), Axial 2 (A2), Centrifugal 1 (C1) and Centrifugal 2 (C2). A1 was operated between 7000 and 13000 rpm at 200-rpm increments. A2 was operated between 8000 and 12000 rpm in 1000-rpm increments. C1 was operated between 800 and 3000 rpm, and C2 was operated between 1800 and 3000 rpm, both at 200-rpm increments.

A novel flow loop (Figure 3.1) was designed to measure pump preload, afterload, and output flow rate under various settings. The loop consisted of two reservoirs filled with a blood-analog fluid (~40% glycerin in water at 36 °C; Hi-Valley

Chemical, Centerville, UT) that had a dynamic viscosity of 3.6 cP. The upper reservoir made use of an adjustable weir to maintain a steady inflow pressure to the LVAD. Connections between components were done with Tygon® tubing (Saint-Gobain, Courbevoie, France). A manual gate valve was placed in series with the LVAD to adjust the resistance (afterload) for each pump speed.

Pump preload, or inflow pressure ($P_i$), and pump afterload, or outflow pressure ($P_o$) were measured with fluid-filled transducers (Edwards LifeSciences, Irvine, CA), and a pressure meter (Living Systems Instrumentation, St. Albans, VT). The pump flow rate (Q) was measured with an ultrasonic flow meter and flow probe (Transonic, Ithaca, NY). Acquisition of flow meter and pressure meter data signals was performed at 40 Hz with a custom system (National Instruments, Austin, TX), and output to a comma separated values (csv) file.

For data analysis and plotting, MATLAB (v6.5; MathWorks, Natick, MA) and a spreadsheet program (Excel 2007, Microsoft, Redmond, WA) were used. The relationship between Q and $\Delta P$ was extracted from the original 40 Hz csv files and tabulated in another spreadsheet file at 0.25-L/min increments for all applicable speeds. Pressure differential across the pump ($\Delta P = P_o - P_i$), which represents the transaortic pressure gradient, was recorded manually in increments of 1 L/min to ensure the integrity of the data acquisition (DAQ) system. PS ($dQ/d\Delta P$) was calculated for all pumps at all speeds using a centered-finite difference approximation at 0.25-L/min increments.

Generic waveforms representing aortic and left-ventricular pressures for fully-loaded LV (minimal to no VAD support), partially-unloaded LV (partial VAD

support), and fully-unloaded (full support with VAD, where AV does not open) were employed to estimate the physiologic pressure gradient (AoP – LVP), which approximated the pressure differential across the pump. The pressure-flow data for each of the four LVADs was then used to estimate their flow rates subject to the hypothetical physiologically varying ΔP. This calculation was done with data from the A1, A2, C1 and C2 LVADs at 9000, 10000, 2000 and 2000 rpm, respectively. Pulsatility index ($Q_{max} - Q_{min} / Q_{avg}$) was also computed for the predicted flow rates. Moreover, PS was gauged as a function of the input cardiac cycle. Pressure sensitivity values and flow rate values were compared with a one-way analysis of variance (ANOVA) technique using 95% confidence intervals. Statistical significance was considered at $p < 0.05$.

### 3.3 Results

Using our novel, open-loop flow system, we demonstrate the characteristic pressure-flow curves obtained for the two axial-flow and two centrifugal VADs (Figure 3.2). Generally, the performance curves for axial-flow devices are steeper and more linear than centrifugal-flow devices. A linear performance curve will maintain constant PS regardless of pressure or flow conditions. The centrifugal-flow pumps have a flat performance curve for low flow rates, and the pressure differential gradually increases for increasing flow. Performance curves for all devices have been characterized for flow rates at pressure differentials down to zero. Also, the line (CLL) along each set of performance curves represents the approximate lower limit of ΔP possible with a closed-loop flow system. Our open-loop flow system is capable of generating ΔP values below that threshold.

Figure 3.3 displays variation in PS for each pump at various pressure differentials and flow rates. As indicative by the performance curves, the PS is greatest at low flow, and continually decreases for increasing flow. The maximum and average PS values for each device across all tested pressure and flow conditions are displayed in Table 3.1. Pressure sensitivity is significantly greater for centrifugal-flow pumps than for axial-flow ($p<0.0001$).

Comparison of two devices at the same impeller speed (e.g., 9000 rpm) is difficult because the hydraulic performance is not likely to be comparable, especially when comparing axial to centrifugal devices. Each device has varying hydraulic performance due to physical characteristics. Thus, characteristic pressure-flow data are collected at a myriad of points in order to establish a baseline impeller speed for each device that yields comparable functionality. For virtual analysis, a speed was selected for each device based on clinical relevance and pressure-flow similarity. The pressure-flow curves for each device at selected speeds are presented in Figure 3.4; A1 at 9000 rpm, A2 at 10000 rpm, and C1 and C2 VADs at 2000 rpm. The displayed performance curves illustrate the variations of hydraulic performance present between various devices, even when pressure-flow values are relatively similar. We find these speeds suitable for comparison.

Additional differences in pump performance were noticed when physiological transaortic pressure gradients were employed for comparison. Figure 3.5 shows three plots. First, aortic and left ventricular pressure waveforms used to estimate $\Delta P$ (AoP – LVP) through the *fully-loaded* cardiac cycle, similar to that explored by Khalil, et al [8]. Second, the flow rates were calculated for the A1, A2, C1 and C2 LVADs given

the fully-loaded cardiac cycle waveform. And third, the PS of the four VADs throughout the cycle. The magnitude of PS through the fully-loaded cycle is ¼x, 1.6x and 2.7x for the A2, C1 and C2 devices, respectively, when compared to the A1 device magnitude. All four devices show highest sensitivity during early diastole, which is marked by the drop in flow rate in center of Figure 3.5. Similarly, Figure 3.6 shows aortic and left ventricular pressure waveforms through the *partially-unloaded* cardiac cycle; the calculated flow rates for the VADs given the partially-unloaded cardiac cycle waveform; and the PS of the four VADs throughout the cycle. As before, the magnitude of PS through the partially-unloaded cycle is ¼x, 0.8x and 5.3x for the A2, C1 and C2 devices, respectively, when compared to the A1 PS magnitude. There is a mean increase of 8% for average flow rate, and a mean reduction of 30% for pulsatility index across all pumps going from fully-loaded to partially-unloaded cycle.

Finally, Figure 3.7 shows aortic and left ventricular pressure waveforms through the *fully-unloaded* cardiac cycle; the calculated flow rates for the VADs given the fully-unloaded cardiac cycle waveform; and the PS of the four VADs throughout the cycle. Again, the magnitude of PS through the fully-unloaded cycle is ¼x, 5x and 15x for the A2, C1 and C2 devices, respectively, when compared to the A1 PS magnitude. There is a mean reduction of 41% and 1% for average flow rate and pulsatility index, respectively, across all pumps going from partially-loaded to fully-unloaded cycle. Of particular interest, the PS of the VADs increases by an average of 66% going from partially-loaded to fully-unloaded cycle. Table 3.2 shows the average flow rate, pulsatility index (PI) and maximum and average PS for each VAD under both the fully-loaded, partially-unloaded and fully-unloaded cardiac cycles.

### 3.4 Discussion

The concept of quantitative PS is exploited here to demonstrate the self-regulating attribute of continuous flow VADs. Here we have demonstrated the capability of our novel, open-loop mock flow structure to generate clinically relevant pressure-flow conditions, heretofore not previously reported in the literature. Indeed, the performance curves go down to pressure differentials equal to zero. Clinically, the extremes are relevant to systole (high flow, uniform pressure), and other physiological conditions that may yield systemic conditions where pump suction or regurgitation may occur. Our data further demonstrate that centrifugal-flow pumps have a greater sensitivity to pressure than the axial-flow pumps, especially in the low and high extremes of flow rate. Finally, we demonstrate that centrifugal pumps demonstrate PS twice that of axial flow devices when exposed to conditions of both partially- or fully-unloaded ventricles.

All pumps exhibit a greater diastolic than systolic sensitivity of pump output (Q) to variations in transaortic pressure gradient. Further, the centrifugal-flow pumps show sensitivities 2-10 times greater than the axial-flow pumps during diastole. Ventricular suction and collapse is a clinically important problem in patients with LVADs. These events most likely occur during end-systole or early-diastole after the ventricle has contracted and the aortic valve has closed (LV isovolumetric relaxation phase), such that both the ventricular volume and internal pressure are minimal. An LVAD that is designed to have high PS during this critical time in the cardiac cycle could reduce the risk of suction, which is observed in the centrifugal pumps, most notably with C2.

Not only can PS imply a reduced risk of suction on the LV, but also suggests an increase in responsiveness during exercise. During exercise, enhanced venous return increases stroke volume and (with increased heart rate) cardiac output that accompany the higher metabolic rates. Any transformation of the venous compliance or peripheral vascular resistance involves a change to the pressure differential across the pump. Devices sensitive to alteration of the pressure differential will naturally respond with a modification of output respective of the external stimulation.

The large magnitudes of PS values in the centrifugal devices are appealing, but must be tempered with clinical issues involved with patient management. In this study, changes in PS correlate with viscosity of the working fluid. That is, higher fluid viscosity correlated to lower PS. As device performance curves are reported in the literature, it is important to note that devices tested in water will exhibit characteristics implying greater PS than if it were tested with a blood-analog fluid of higher viscosity. Clinically, this also has an effect on the device performance over time. For example, when a patient's hematocrit is low, the output of the pump will be more sensitive to variations in system pressure.

One feature of this study that is unique with regards to device testing is demonstrating the performance and behavior of each VAD under clinically-relevant situations: loaded, partially-unloaded, and fully-unloaded conditions, respectively. While some patients require full unloading to provide necessary support, the majority of VAD patients likely live in a partially-unloaded state, whereby the VAD would reduce the maximum LVP level, but still allow the AV to open during systole [12]. Under this condition the pressure differential would reach a state of equilibrium ($\Delta P =$

0). Unloading the heart has been shown to have beneficial effects on LV function by improving cardiothoracic ratio, decreasing heart size, and increasing circulation [9]. Moving from a fully-loaded to a partially-unloaded condition gives way to moderate changes in pump performance, with a minimal increase in average flow, and 33% decrease of pulsatility index. That said, we observed several, relevant distinguishing features between partially-unloaded and fully-unloaded ventricle conditions. The maximum LVP level during a fully-unloaded condition is significantly lower than AoP, thus, not allowing the AV to open. With the AV closed, the transaortic pressure gradient never reaches zero.

Both partial and full unloading resulted in sizeable decreases in average flow for all devices, and a substantial increase in average PS. C1 experiences the greatest relative increase of average PS, and interestingly, a relative increase in PS magnitude, which no other device exhibits. The average PS for A1, A2 and C2 also increase, but the magnitude, or range, of sensitivity values decreases. This is most likely due to the shape of the observed performance curve for each device at the applied range of pressure differentials for a fully-unloaded condition.

Our data must be interpreted with several caveats. Clinically speaking, when a LVAD is initially connected to the circulatory system in a patient with end-stage heart failure, the ventricle is most likely to experience a fully-unloaded condition. As the ventricle recovers, it could move to the partially-unloaded condition. Here, the device-centric analyses highlight a single operating speed for each device. However, we recognize that a partially-unloaded condition may occur at a lower operating VAD speed than that of a fully-unloaded condition. We felt it most significant to look at

each device at a single operating speed for this study. Further studies could be executed to model PS, flow and pulsatility as a function of speed.

### 3.5 Conclusions

In summary, the present study demonstrates that continuous flow VADs self-regulate performance by adjusting device output via their individual sensitivity to pressure differential. We further show that although centrifugal-flow devices have similar PS to the axial-flow devices at higher flow rates (6-8 L/min), they have a significant difference in PS at intermediate to low flow rates, including those near standard physiological conditions. Further enhancements to PS could lead to self-regulation of device output such that the pump would mimic the natural response of the native heart under exercise and rest conditions, as well as minimize undesirable effects such as LV wall suction or atrial collapse.

### 3.6 References

1. Guyton AC, Hall JE. Textbook of Medical Physiology, 12th ed. Saunders; 2011.

2. Joyce DL, Joyce LD, Loebe M. Mechanical Circulatory Support: Principles and Applications. McGraw-Hill; 2011.

3. Kormos RL, Miller LW. Mechanical Circulatory Support: A Companion to Braunwald's Heart Disease. Elsevier; 2011.

4. Nose Y. Is a pulsatile cardiac prosthesis a dying dinosaur? Artif Organs 1992; 16:233-234.

5. Saxton GA Jr, Andrews CB. An ideal heart pump with hydrodynamic characteristics analogous to the mammalian heart. ASAIO Trans 1960; 6:288-291.

6. Akimoto T, Yamazaki K, Litwak P, et al. Relationship of blood pressure and pump flow in an implantable centrifugal blood pump during hypertension. ASAIO J 2000; 46:596-599.

7. Akimoto T, Yamazaki K, Litwak P, et al. Rotary blood pump flow spontaneously increases during exercise under constant pump speed: results of a chronic study. Artif Organs 1999; 23:797-801.

8. Khalil HA, Cohn WE, Metcalfe RW, Frazier OH. Preload sensitivity of the Jarvik 2000 and HeartMate II LVADs. ASAIO J 2008; 54:245-248.

9. Salamonsen RF, Mason DG, Ayre PJ. Response of rotary blood pumps to changes in preload and afterload at a fixed speed setting are unphysiological when compared with the natural heart. Artif Organs 2011; 35:E47-53.

10. Frazier OH, Khalil HA, Benkowski RJ, Cohn WE. Optimization of axial-pump pressure sensitivity for a continuous-flow TAH. J Heart Lung Transplant 2010; 29:687-91.

11. Farrar DJ, Bourque K, Dague CP, Cotter CJ, Poirier VL. Design features, developmental status and experimental results with the Heartmate III centrifugal LVAS with magnetically levitated rotor. ASAIO J 2007; 53:310-15.

12. Mizuno T, Weisel RD, Li RK. Reloading the heart: a new animal model of LVAD removal. J Thorac Cardovasc Surg 2005; 130:99-106.

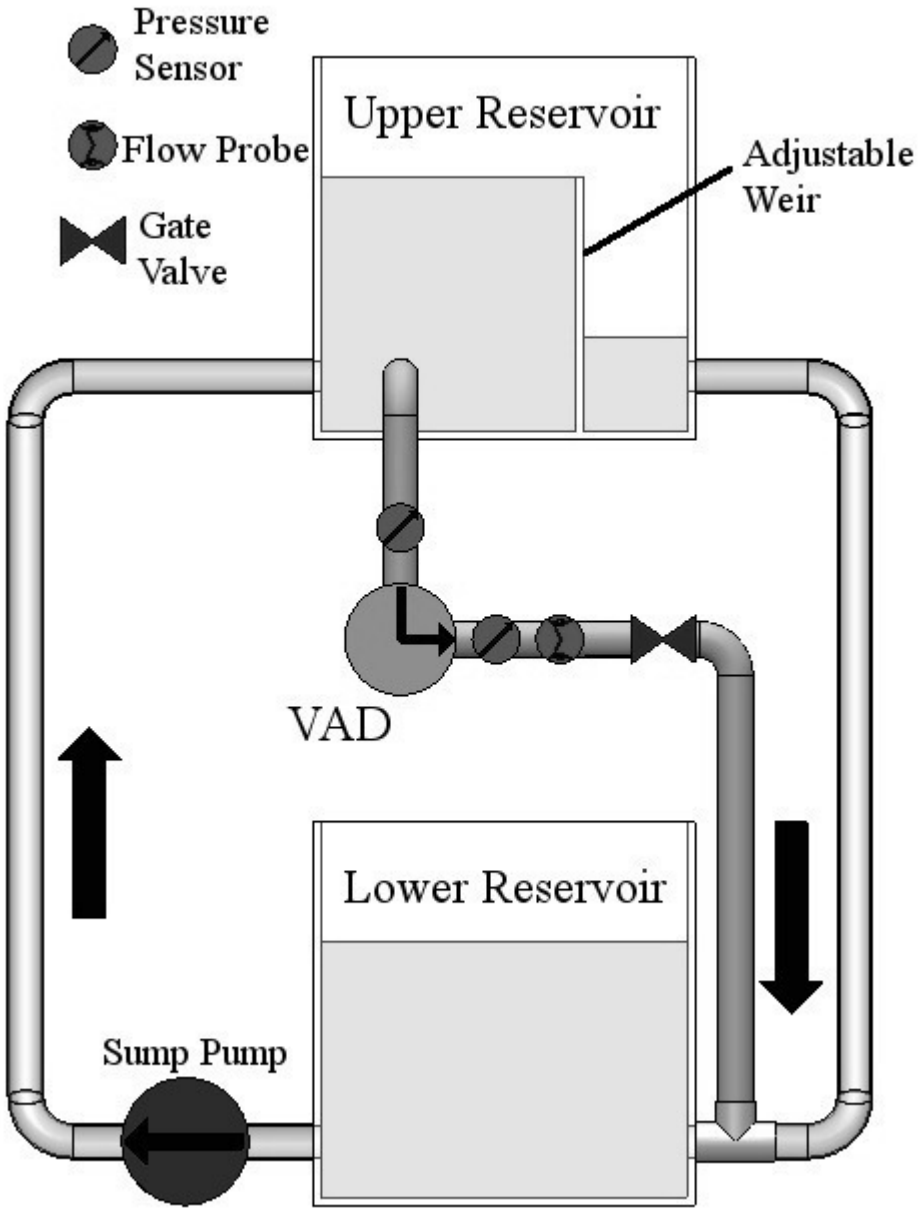


Figure 3.1. Novel open-loop flow system designed to impose low and high extremes of pressure differential on tested ventricular assist devices (VADs).

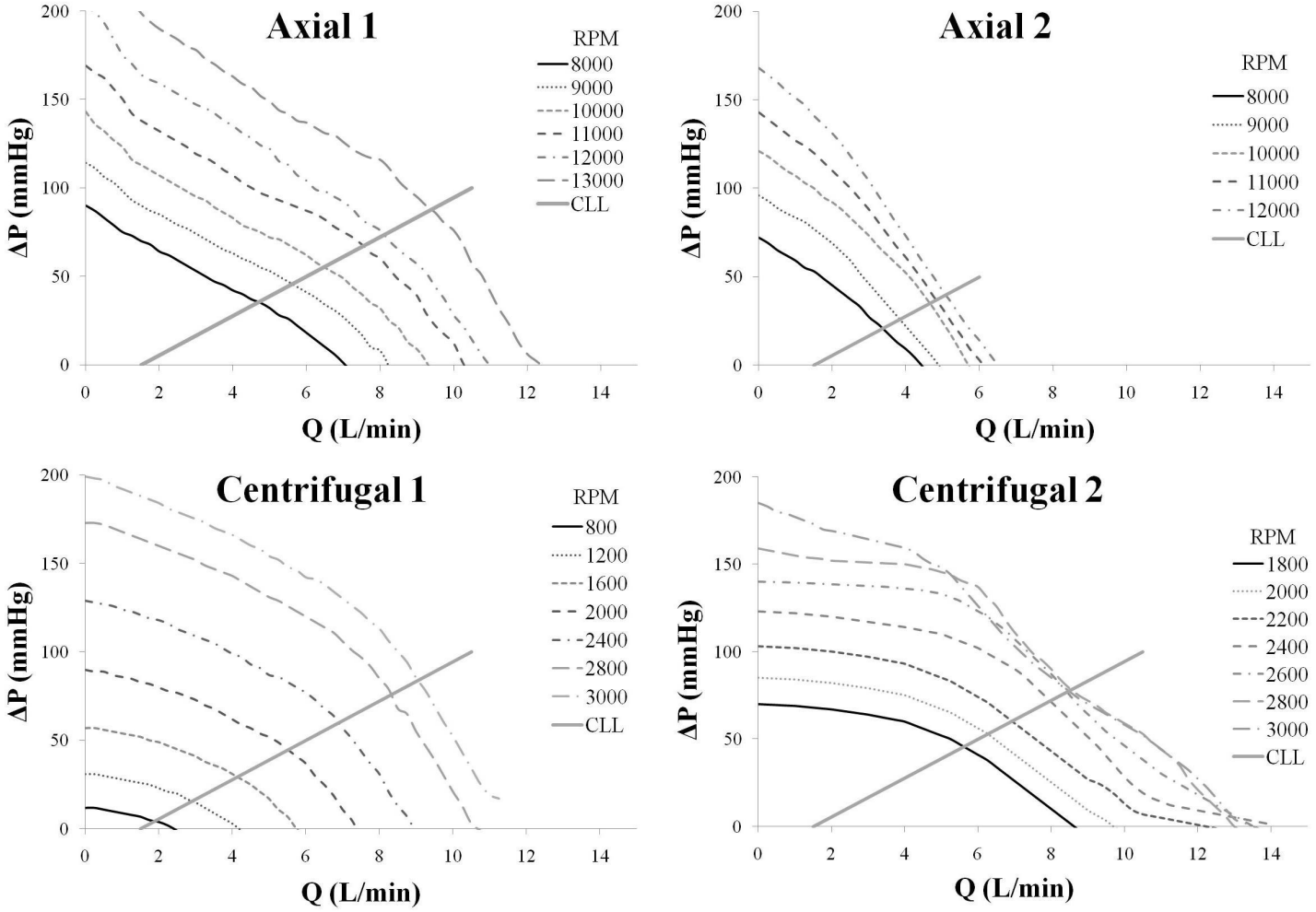


Figure 3.2. Characteristic pressure-flow curves for the axial (A1, A2) and centrifugal (C1, C2) VADs. *ΔP*, pressure differential; *Q*, pump flow rate; *CLL*, closed-loop limit.

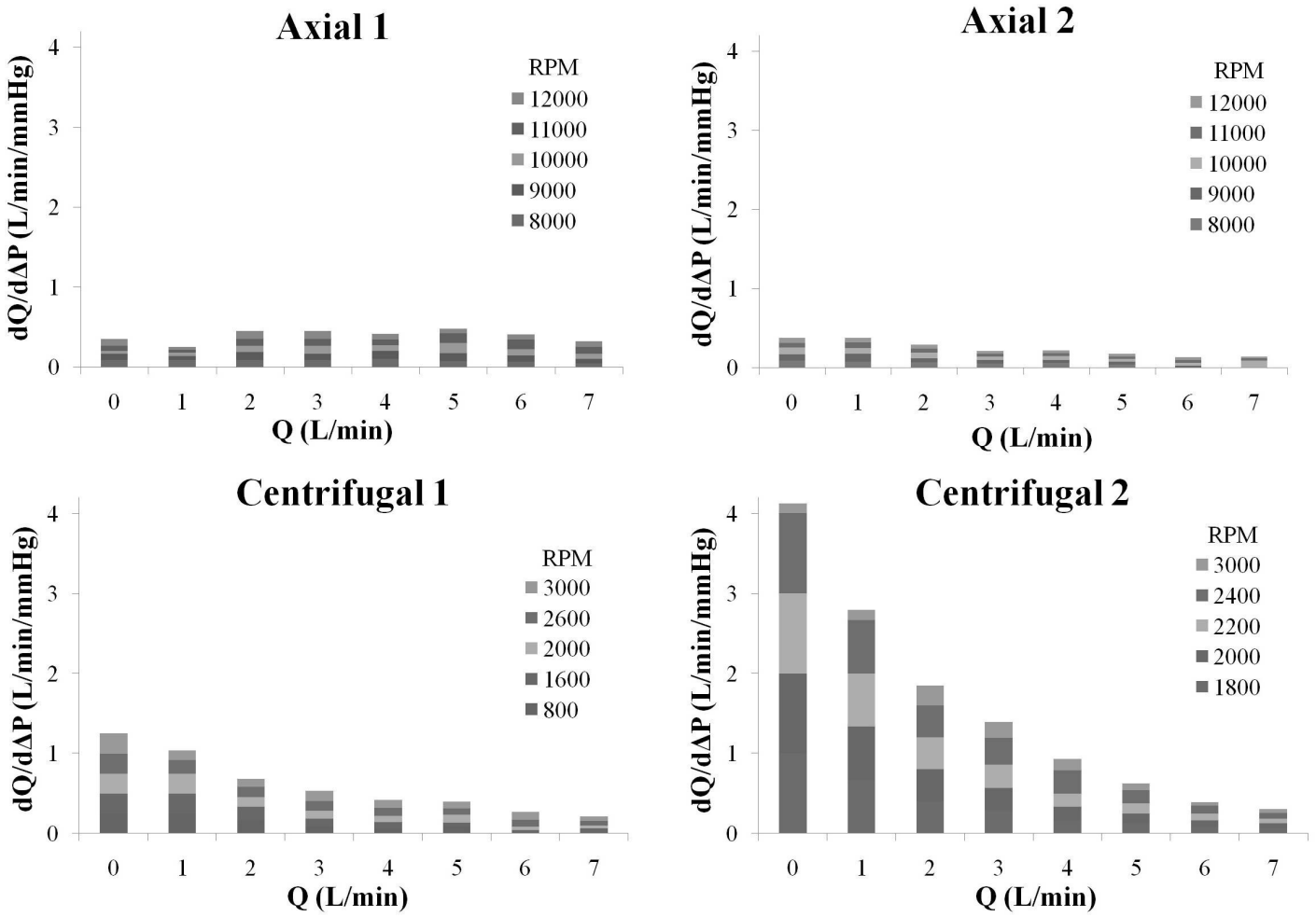


Figure 3.3. Pressure sensitivity for the axial (A1, A2) and centrifugal (C1, C2) VADs. *dQ/dΔP*, pressure sensitivity; *Q*, pump flow rate.

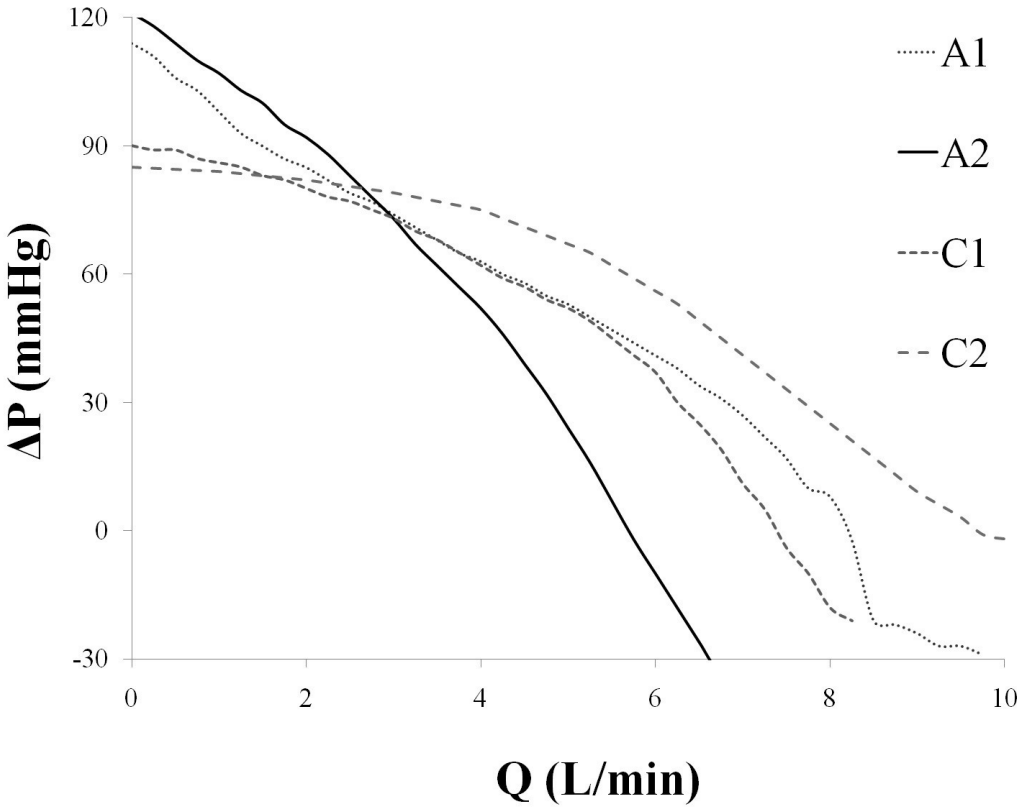


Figure 3.4. Characteristic pressure-flow curves for A1 at 9000 rpm, A2 at 10,000 rpm, and C1 and C2 VADs at 2000 rpm. *ΔP*, pressure differential; *Q*, pump flow rate.

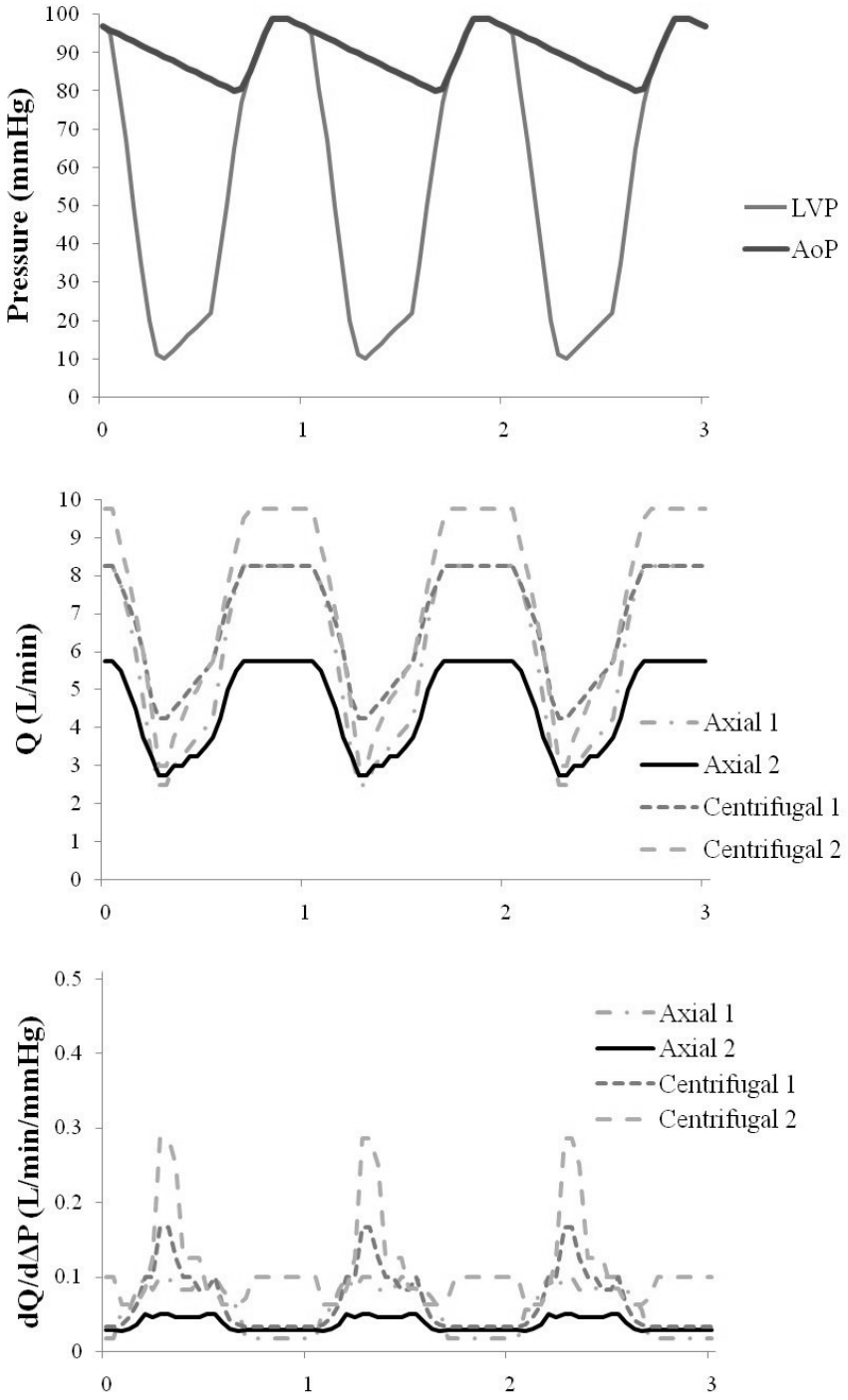


Figure 3.5. Aortic pressure (AoP) and left ventricular pressure (LVP) in a fully-loaded ventricle (A). Calculated flow rates for A1 at 9000 rpm, A2 at 10,000 rpm, and C1 and C2 VADs at 2000 rpm (B). *Q*, pump flow rate. Variation in pump pressure sensitivity (L/min/mmHg) during the cardiac cycle (C). *dQ*/*dΔP*, pressure sensitivity.

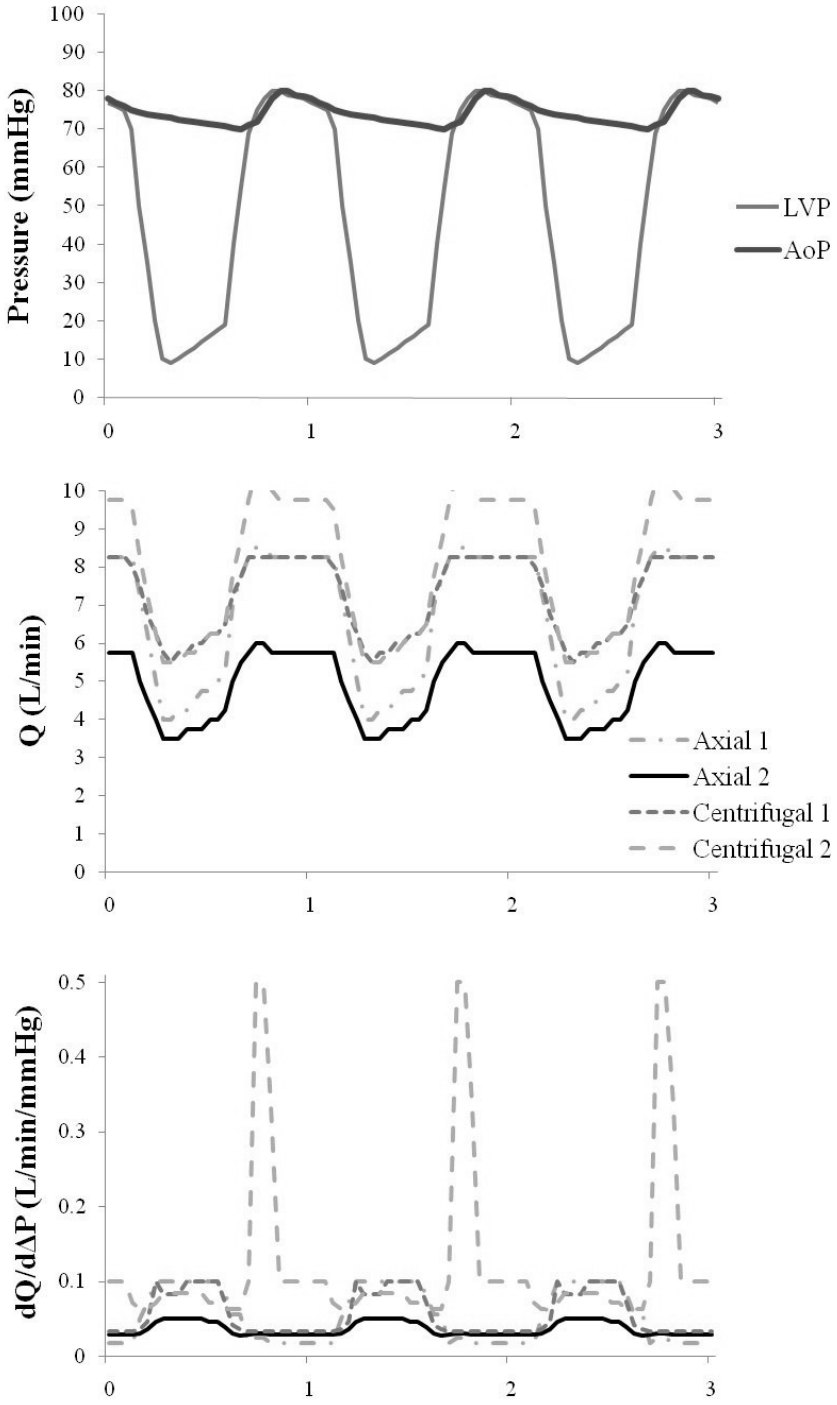


Figure 3.6. Aortic pressure (AoP) and left ventricular pressure (LVP) in a partially-unloaded ventricle (A). Calculated flow rates for A1 at 9000 rpm, A2 at 10,000 rpm, and C1 and C2 VADs at 2000 rpm (B). *Q*, pump flow rate. Variation in pump pressure sensitivity (L/min/mmHg) during the cardiac cycle (C). *dQ*/*dΔP*, pressure sensitivity.

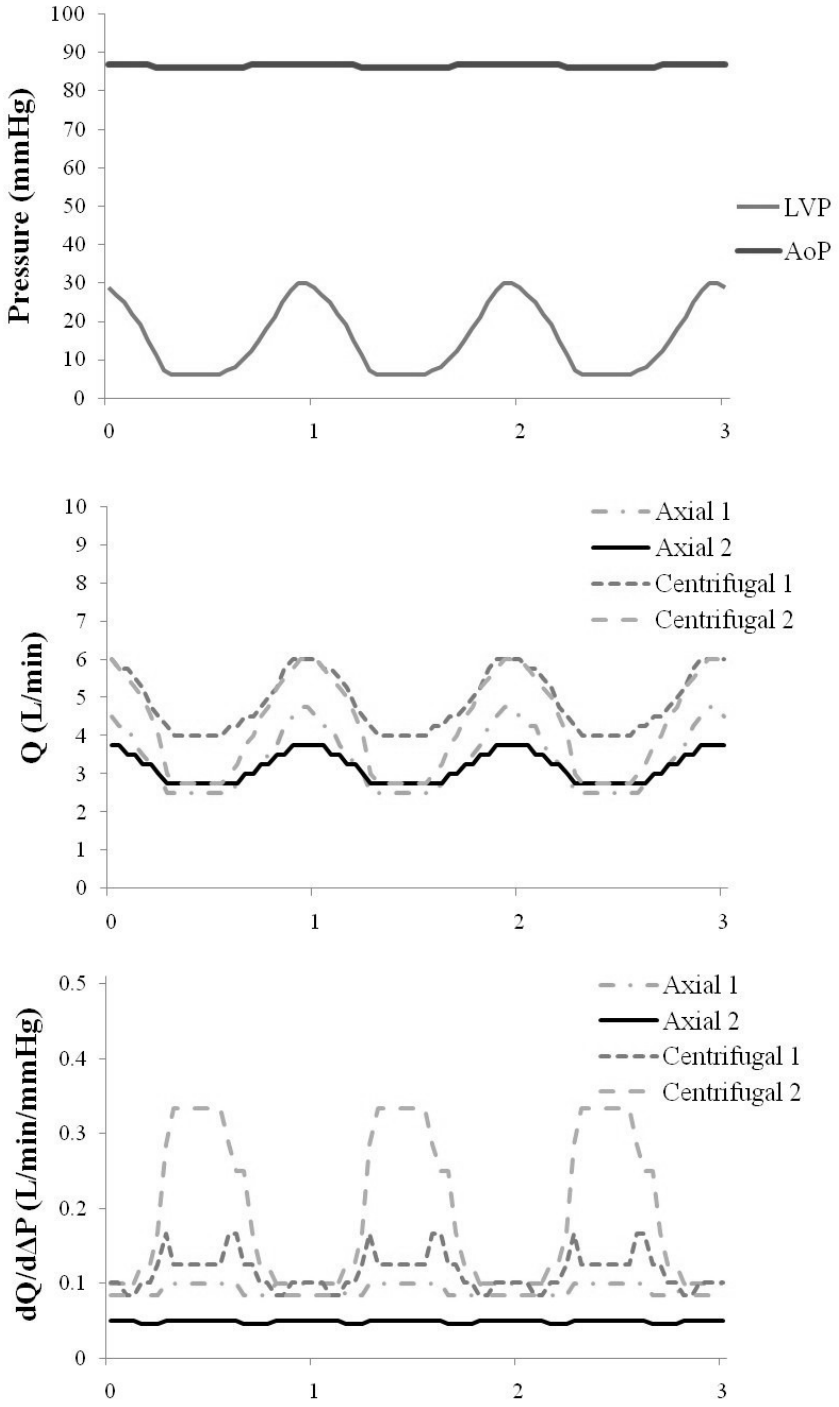


Figure 3.7. Aortic pressure (AoP) and left ventricular pressure (LVP) in a fully-unloade ventricle (A). Calculated flow rates for A1 at 9000 rpm, A2 at 10,000 rpm, and C1 and C2 VADs at 2000 rpm (B). *Q*, pump flow rate. Variation in pump pressure sensitivity (L/min/mmHg) during the cardiac cycle (C). *dQ*/*dΔP*, pressure sensitivity.

Table 3.1. Maximum and average pressure sensitivity (PS) values for each ventricular assist device across all tested pressure and flow conditions. Average values are presented with standard deviations (SD).

| | **Axial 1 (A1)** | **Axial 2 (A2)** | **Centrifugal 1 (C1)** | **Centrifugal 2 (C2)** |
|---|---|---|---|---|
| Max PS | .13 | .10 | .25 | 1.00 |
| Avg PS | .08±.02 | .05±.02 | .12±.08 | .28±.34 |
| *p* | .02 | <.0002 | <.02 | <.0002 |

Table 3.2. Maximum and average pressure sensitivity (PS) values, average flow rate, pulsatility index (PI) for each VAD under the fully-loaded, partially-unloaded and fully-unloaded cardiac cycles. Percent change for average pressure sensitivity, average flow and pulsatility index going from partially- to fully-unloaded condition. Average values are presented with standard devations (SD).

| Condition | Device | **Axial 1 (A1)** | **Axial 2 (A2)** | **Centrifugal 1 (C1)** | **Centrifugal 2 (C2)** |
|---|---|---|---|---|---|
| | Impeller speed (RPM) | **9000** | **10000** | **2000** | **2000** |
| fully-loaded | Max PS (L/min/mmHg) | .10 | .05 | .17 | .29 |
| | Avg PS ($p$<.0001) | .06±.03 | .04±.01 | .07±.04 | .11±.06 |
| | Avg Flow (L/min) ($p$<.0001) | 6.1±2.2 | 4.6±1.2 | 6.8±1.5 | 7.3±2.4 |
| | Pulsatility Index (PI) | 0.9 | 0.7 | 0.6 | 0.9 |
| partially-unloaded | Max PS | .10 | .05 | .10 | .50 |
| | Avg PS ($p$<.0001) | .05±.04 | .04±.01 | .06±.03 | .12±.12 |
| | Avg Flow ($p$<.0001) | 6.7±1.8 | 4.9±0.9 | 7.2±1.1 | 8.1±1.9 |
| | Pulsatility Index | 0.7 | 0.5 | 0.4 | 0.6 |
| fully-unloaded | Max PS | .10 | .05 | .17 | .33 |
| | Avg PS ($p$<.0001) | .10±.01 | .05±.00 | .11±.02 | .19±.11 |
| | Average Flow ($p$<.0001) | 3.3±0.8 | 3.2±0.4 | 4.9±0.8 | 4.3±1.3 |
| | Pulsatility Index | 0.7 | 0.3 | 0.4 | 0.8 |
| Percent change | Avg PS | +74 | +33 | +102 | +55 |
| | Avg Flow | -50 | -35 | -33 | -47 |
| | Pulsatility Index | 0 | -38 | +8 | +24 |

# CHAPTER 4

# IN VITRO PULSATILITY ANALYSIS OF AXIAL-FLOW AND CENTRIFUGAL-FLOW LEFT VENTRICULAR ASSIST DEVICES

Recently, continuous-flow ventricular assist devices (CF-VADs) have supplanted older, pulsatile-flow pumps, for treating patients with advanced heart failure. Despite the excellent results of the newer generation devices, the effects of long-term loss of pulsatility remain unknown. The aim of this study is to compare the ability of both axial and centrifugal continuous-flow pumps to intrinsically modify pulsatility when placed under physiologically diverse conditions. Four VADs, two axial- and two centrifugal-flow, were evaluated on a mock circulatory flow system. Each VAD was operated at a constant impeller speed over three hypothetical cardiac conditions: normo-tensive, hypertensive, and hypotensive. Pulsatility index (PI) was compared for each device under each condition. Centrifugal-flow devices had a higher PI than that of axial-flow pumps. Under normo-tension, flow PI was 0.98 ± 0.03 and 1.50 ± 0.02 for the axial and centrifugal groups, respectively ($p < 0.01$). Under hypertension, flow PI was 1.90 ± 0.16 and 4.21 ± 0.29 for the axial and centrifugal pumps, respectively ($p = 0.01$). Under hypotension, PI was 0.73 ± 0.02 and 0.78 ± 0.02 for the axial and centrifugal groups, respectively ($p = 0.13$). All tested CF-VADs

were capable of maintaining some pulsatile-flow when connected in parallel with the mock ventricle. It is concluded that centrifugal-flow devices outperform the axial pumps from the basis of PI under tested conditions.

## 4.1 Introduction

Mechanical circulatory support is an important and increasingly prevalent therapy for patients with advanced heart failure. Ventricular assist devices (VADs) are broadly distinguished as either volume-displacement (pulsatile-) or continuous-flow pumps. The advantages and disadvantages of pulsatile versus non-pulsatile blood flow have been chronicled and deliberated for decades [1,2]. However, the acceptance and increasing use of continuous-flow systems has come about by ongoing research demonstrating excellent recovery of failing end-organs and enhanced survival [3-5]. Rotary VADs have alleviated several concerns that earlier volume-displacement pumps experienced, including efficiency [6], anatomic fit [7], durability [8], hemolysis [9], and reliability [10]. Physically, the continuous-flow pumps have traded in a decrease in pulse pressure for a smaller sized device. With the lasting effects of chronic non-pulsatile flow unknown and the wide spread and increasing use of these devices, examination of VAD responses to inherent fluctuations in preload and afterload, and performance during moderate pulsatile-flow is clinically relevant.

As the designs of CF-VADs continue to evolve, maintaining or producing pulsatile flow is a sought-after positive feature. Quantifying the level of pulsatile-flow through a CF-VAD establishes a metric by which different devices can be compared. Pulsatility index (PI) is defined as a measurement for variability of the fluid flow rate.

PI is calculated to relate devices to the level of pulsatile flow that is generated under a given condition. Some CF-VADs report PI on the system monitor and use it for speed control [11,12]. Even if PI is not reported, an estimated flow rate usually is, so it is possible to estimate PI as the amplitude in flow rate varies.

This author and others have observed clinically that various CF-VADs are capable of greater PI than others. To date, however, no reports exist that experimentally contrast multiple continuous-flow devices under pulsating-type, hence physiologic, conditions. Comparison of implanted devices involves too many variables for direct scientific analysis, and if attempted would require a very large sample group to be statistically viable. *In vitro* experiments designed to analyze VAD performance under pulsating pressure and flow will show how they compare to one another under physiologic conditions. Clinically, we are faced with real, important challenges in patient management based on both the loading (volume status) and unloading (hypertension) conditions of the ventricle. This study investigates the variations in *in vitro* pulsatility characteristics generated by four CF-VADs, two axial-flow type and two centrifugal- (or radial-flow) design.

## 4.2 Methods

The mock circulation system (Figure 4.1) consists of atrium (LA), ventricle (LV), and lumped systemic (SCC) and pulmonary (PCC) compliance/resistance chambers, similar to that described by Pantalos, *et al.* [13], hybridized with the open-loop flow system described in Chapter 2. Both artificial atrium and ventricle are made of flexible polyurethane sacs, with the ventricular sac housed in a pressurization

chamber. The ventricle top supports mounting for inflow (mitral) and outflow (aortic) prosthetic valves. Porcine pericardial valves (Baxter, Deerfield, IL) are employed for this experiment. Contraction and pulsatile flow is sustained by connection of the ventricular chamber to a pneumatic controller. Additionally, the loop employs reservoirs filled with a blood-analog fluid (~40% glycerin in water at 36 °C; Hi-Valley Chemical, Centerville, UT) with a dynamic viscosity of 3.6 cP. All connections between chambers and reservoirs are made using Tygon® tubing (Saint-Gobain, Courbevoie, France). A manual gate valve was placed after the SCC to adjust the resistance (afterload).

With the mock circulation loop capable of pulsatile pressure and flow, VADs are tested by simulated LV apex cannulation and aortic anastomosis. The devices under analysis are referred to as Axial 1 (A1), Axial 2 (A2), Centrifugal 1 (C1) and Centrifugal 2 (C2). Investigation is carried out on each device under three pulsatile conditions: normo-tensive, hypertensive, and hypotensive. Pressure values significant and adjustable to each cardiac condition are displayed in Table 4.1. All three conditions maintain a uniform beat rate of 100 beats per minute (bpm), and a stiff systemic compliance of 0.5 mL/mmHg.

The pump flow rate (Q) was measured with an ultrasonic flow meter and flow probe (Transonic, Ithaca, NY). Pump preload, or inflow pressure ($P_i$), and pump afterload, or outflow pressure ($P_o$) are measured with fluid-filled transducers (Edwards LifeSciences, Irvine, CA), and a pressure meter (Living Systems Instrumentation, St. Albans, VT). Acquisition of flow meter and pressure meter data signals was

performed at 40 Hz with a custom system (National Instruments, Austin, TX). For data analysis and plotting, MATLAB (v6.5; MathWorks, Natick, MA) and a spreadsheet program (Excel 2007, Microsoft, Redmond, WA) were used.

Each analysis is done at a single impeller speed for each pump. Because of the inherent differences between axial- and centrifugal-flow pumps, running all four devices at the same speed (rpm) is not feasible for allowing suitable comparisons. Thus, speeds were selected for each pump that had been previously determined by comparison of pressure-flow performance curves, as well as clinical experience (Chapter 3). Speeds selected for A1, A2, C1 and C2 pumps were 9000, 10000, 2000 and 2000 rpm, respectively.

### 4.3 Calculations

A portion of the captured data yields a set of points showing the variability of flow rate over time. The data will be used to calculate pulsatility index for flow ($PI_Q$), which is the difference between maximum and minimum flow rates divided by the average flow rate, or equation 4.1. Choi, *et al.* described another useful pulsatility metric as the pulsatility ratio [14,15]. The pulsatility ratio ($R_{pul}$) is a ratio of pulsatility indices for flow and pressure ($R_{pul} = PI_Q / PI_{\Delta P}$). For this the preload and afterload data points were used to compute a pressure differential waveform against time. From the pressure differential waveform, a pulsatility index for pressure differential ($PI_{\Delta P}$) will be computed via equation 4.2. The calculations described here will be used to assess the level of pulsatile flow that the analyzed continuous-flow devices are able to generate while connected in parallel with a synthetic heart.

$$PI_Q = \frac{Q_{\max} - Q_{\min}}{Q_{avg}} \quad (4.1)$$

$$PI_{\Delta P} = \frac{\Delta P_{\max} - \Delta P_{\min}}{\Delta P_{avg}} \quad (4.2)$$

Continuous flow rate and pressure differential data are presented as mean ± SD. Percentages are used for categorical data. Results were compared by *t*-test or by one-way analysis of variance (ANOVA). Statistical significance was considered at $p < 0.05$.

## 4.4 Results

Initially, it was determined to be necessary to create a physiologic *in vitro* model system that allows for the dynamic, rather than static, testing of the axial- and centrifugal-flow devices. Figure 4.2 graphically depicts three clinically-relevant conditions: normo-tensive, hypertensive, and hypotensive. As demonstrated, the peak systolic left ventricular pressure (LVP) exceeds the nominal aortic pressure (AoP) signifying that the aortic valve (AV) continues to open for all three conditions. Opening of the AV during VAD implantation may also be referred to as partial-support, as opposed to full-support, where the AV does not open. The first condition, normo-tensive, was selected as a partial-support baseline. The second and third conditions are high and low variations, respectively, for relative pressures. As expected, the hypertensive case shows the largest diastolic pressure differentials of the three, with the hypotensive case showing the smallest. All four pumps were subjected to each of the three pulsatile cardiac conditions on the mock circulation loop.

The pulsatile Q and ΔP waveforms measured on each device under all conditions on the mock loop are shown in Figures 4.3 – 4.5. The waveforms are displayed over a brief three-second window during the operation of each device. With all devices the peak in Q coincides with the dip in ΔP. Thus, highest flow occurs during systole when the AV is open and the transaortic pressure gradient is minimal. Data from the waveforms is used to compute pulsatility characteristics, which are presented in Table 4.2.

Under the normo-tensive condition, (Figure 4.3), the average Q for axial devices is slightly greater (10%) than centrifugal ones; however, the $PI_Q$ and $R_{pul}$ is much greater for centrifugal devices. $PI_Q$ was 0.98 ± 0.03 and 1.50 ± 0.02 for the axial and centrifugal groups, respectively ($p < 0.01$). Similarly, Figures 4.4 and 4.5 show pulsatile Q and ΔP waveforms for each pump under the hypertensive and hypotensive models, respectively. A point of interest under the hypertensive case shows that both centrifugal devices experience negative, or reverse flow, also known as pump regurgitation. Negative flow can have a significant impact on the physiological system, as well as on computation of PI. $PI_Q$ and $R_{pul}$ of centrifugal devices under hypertension is double that of the axial pumps. $PI_Q$ was 1.90 ± 0.16 and 4.21 ± 0.29 for the axial and centrifugal groups, respectively ($p = 0.01$).

No statistical significance was seen when comparing the Q or ΔP under normo-tensive or hypertensive conditions. However, hypotension shows variation in mean Q and ΔP for A2 (further illustrated in Figure 4.6). The similarity between Q and ΔP yields $PI_Q$ that is nearly uniform between the pumps: 0.73 ± 0.02 and 0.78 ±

0.02 for the axial and centrifugal groups, respectively ($p = 0.13$). Interestingly, $R_{pul}$ for the centrifugal devices remain above those yielded by axial-flow pumps. $R_{pul}$ was 0.50 ± 0.05 and 0.77 ± 0.06 for the axial and centrifugal groups, respectively ($p < 0.04$).

Figure 4.6 presents the ΔP and Q relationship for each device under all three simulated cardiac conditions. The pressure-flow performance curve for each device follows a clockwise loop, with systole covering the right and lower portions of the loop and diastole over the left and upper sections. The size of a performance loop is directly related to the amount of hydraulic power supplied by each device. Hydraulic power, calculated by integrating the area within the performance loops, is displayed in Figure 4.7. All devices show distinctively greater power in hypertension, and lower power in hypotension. A1 is markedly lower than the other three devices in all conditions, except for C1 under hypertension. However, power differences between the groups (axial vs. centrifugal) are not statistically significant.

## 4.5 Discussion

The common goal of all VADs is to augment systemic cardiac output and reduce the load on the ventricle during the cardiac cycle without leading to significant biological or hematological complications. Accomplishing this goal while maintaining evolutionarily-preserved physiology, i.e., pulsatility, may influence the ability of these devices to provide beneficial and durable support for the advanced heart failure patient. Comparative efficacy of pulsatile- and continuous-flow VADs have extensively documented their effects on ventricular unloading [16,17], hemodynamics [18,19], end organ function and microcirculation [20], as well as vascular reactivity

[21]. While continuous-flow devices are not pulsatile by design, it is hereby shown that some designs exhibit the ability to be more pulsatile than others.

This study compares pulsatility characteristics of two axial-flow and two centrifugal-flow VADs under varying physiologic conditions. The centrifugal-flow device design is shown to produce greater pulsatile flow than the axial-flow device, when connected in parallel with a synthetic, pulsating ventricle. The difference is most notable under low-flow, high-pressure circumstances, which agree with typical design environment settings for centrifugal-flow pumps [22].

Further, this study shows that pulsatility ratio is higher in the centrifugal rather than the axial-flow devices. Choi, *et al.* show that ventricular suction events occur with a decrease in $R_{pul}$, and state that it is a more reliable metric to mitigate suction events than is the $PI_Q$ metric [14]. It is hereby postulated that $R_{pul}$ can be employed as a qualitative metric to predict which device design will be more or less prone to alleviate suction events. Ultimately, suction events are a function of patient anatomy, physiological condition, inflow orientation and more. However, $R_{pul}$ should be considered as a viable metric that may abate the occurrence of such events.

The influence of VAD therapy on positive cardiac remodeling and improvement in LV function remains an active, and often disputed, field of investigation [23,24]. It is unknown to what extent the differences observed in $PI_Q$ between the axial-flow pumps and centrifugal-flow pumps have on the potential for LV recovery. Recovery is thought to be associated with unloading the LV. However, long-term full-support, or complete unloading, where the aortic valve ceases to open

during the cardiac cycle, may lead to muscle atrophy. This study does not consider the full-support case, to which many VAD recipients are subject immediately after implantation. This study only considers partial-support for all analyzed cardiac conditions, which may be preferred for long-term support. More volume unloading could have been achieved by increased impeller speed in each device; however, speeds common to current clinical implementation were employed.

The ΔP-Q performance loop illustrates the considerable distinction between systole and diastole that a pump experiences during implantation. Typical *in vitro* analysis, under continuous-flow conditions, yields pressure-flow performance to be a single curve for a given impeller speed [25]. However, this study shows that the clinical application of the continuous-flow rotary pump connected in parallel with a pulsing system yields a noticeably altered performance curve, or in this case, performance loop. This illustrates the dynamic environment to which the VAD is subject. End-diastole to early-systole appears to be similar to steady-state hydrodynamic performance curves in most cases, but end-systole to early-diastole is divergent. With LVP alternately increasing and decreasing throughout the cardiac cycle, the output variable(s) [Q, AoP] form a rate-dependent hysteresis loop. The hysteresis loop occurs due to the relative sinusoidal waveform oscillations of ΔP and Q being out of phase with one another: that is, ΔP increases while Q decreases, and vice versa, which is due to overall dynamic lag in the system. The lag is due, in part, to the compliant nature of the various chambers throughout the experimental test loop.

Analogous alteration of pressure and flow is expected to be present in the implanted configuration.

## 4.6 Conclusion

In conclusion, this study indicates that both axial and centrifugal continuous-flow pump designs maintain some pulsatile flow when connected in parallel with the ventricle. Of the two designs, the centrifugal-flow provides significantly greater pulsatility index when exposed to physiologic conditions of varying preload and afterload. Further, the pulsatility ratio exhibited by the centrifugal-flow designs lead us to believe that they are more likely to abate suction events. Improved response to changes in left ventricular pressure may continue to increase pulsatility of continuous-flow devices.

## 4.7 References

1. Wesolowski SA, Fisher JH, Welsh CS. Perfusion of the pulmonary circulation by nonpulsatile flow. Surgery 1953; 33:370-375.

2. Nose Y. Is a pulsatile cardiac prosthesis a dying dinosaur? Artif Organs 1992; 16:233-234.

3. Hindman BJ, Dexter F, Ryu KH, Smith T, Cutkomp J. Pulsatile versus nonpulsatile cardiopulmonary bypass: no difference in brain blood flow or metabolism at 27 [degrees] C. Anesthesiology 1994; 80:1137-1147.

4. Pagani FD, Miller LW, Russell SD, et al. Extended mechanical circulatory support with a continuous-flow rotary LVAD. J Am Coll Cardiol 2009; 54:312-321.

5. Slaughter MS, Rogers JG, Milano CA, et al. Advanced heart failure treated with continuous-flow LVAD. N Engl J Med 2009; 361:2241-2251.

6. Nose Y. The need for a nonpulsatile pumping system. Artif Organs 1988; 12:113-115.

7. Unger F. Review article: Current status and use of artificial hearts and circulatory assist devices. Perfusion 1986; 1:155-163.

8. Olsen DB. The history of continuous-flow blood pumps. Artif Organs 2000; 24:401-404.

9. Allen GS, Murray KD, Olsen DB. The importance of pulsatile and nonpulsatile flow in the design of blood pumps. Artif Organs 1997; 21:922-928.

10. Potapov EV, Loebe M, Nasseri BA, Sinawski H, Koster A, Kuppe H, et al. Pulsatile flow in patients with a novel nonpulsatile implantable VAD. Circulation 2000; 102:III-183–III-187.

11. Griffith BP, Kormos RL, Borovetz HS, et al. HeartMate II LVAS: from concept to first clinical use. Ann Thorac Surg 2001; 71:S116-S120.

12. Choi S, Antaki JF, Boston JR, Thomas DA. Sensorless approach to control of a turbodynamic LVAS. IEEE T Contr Syst T 2001; 9:473-82.

13. Pantalos GM, Koenig SC, Gillars KJ, Giridharan GA, Ewert DL. Characterization of an adult mock circulation for testing cardiac support devices. ASAIO J 2004; 50:37-46.

14. Choi S, Boston JR, Antaki, JF. An investigation of the pump operating characteristics as a novel control index for LVAD control. International Journal of Control, Automation, and Systems 2005; 3:100-108.

15. Choi S, Boston JR, Antaki JF. Hemodynamic controller for LVAD based on pulsatility ratio. Artif Organs 2007; 31:114-125.

16. Garcia S, Kandar F, Boyle A, et al. Effects of pulsatile- and continuous-flow LVADs on left ventricular unloading. J Heart Lung Transplant 2008; 27:261-7.

17. Klotz S, Deng M, Stypmann J, et al. Left ventricular pressure and volume unloading during pulsatile versus nonpulsatile LVAD support. Ann Thorac Surg 2004; 77:143–50.

18. Haft J, Armstrong W, Dyke DB, et al. Hemodynamic and exercise performance with pulsatile and continuous-flow LVADs. Circulation 2007; 116:I-8-15.

19. DiGiorgi PL, Smith DL, Naka Y, Oz MC. In vitro characterization of aortic retrograde and antegrade flow from pulsatile and nonpulsatile VADs. J Heart Lung Transplant 2004; 23:186–92.

20. Nakata K, Shiono M, Hata M, et al. Effect of pulsatile and nonpulsatile assist on heart and kidney microcirculation with cardiogenic shock. Artif Organs 1996; 6:681– 4.

21. Amir O, Radovancevic B, Delgado R, et al. Peripheral vascular reactivity in patients with pulsatile vs. axial flow LVAD support. J Heart Lung Transplant 2006; 25:391–4.

22. Stepanoff AJ. Centrifugal and Axial Flow Pumps: Theory, Design, and Application. Wiley; 1948.

23. Young JB. Healing the heart with VAD therapy: mechanisms of cardiac recovery. Ann Thorac Surg 2001; 71:S210 –S219.

24. Levin H, Oz M, Chen J, Packer M, Rose E, Burkhoff D. Reversal of chronic ventricular dilatation in patients with end-stage cardiomyopathy by prolonged mechanical unloading. Circulation 1995; 91:2717–2720.

25. Farrar DJ, Bourque K, Dague CP, Cotter CJ, Poirier VL. Design features, developmental status and experimental results with the Heartmate III centrifugal LVAS with magnetically levitated rotor. ASAIO J 2007; 53:310-15.

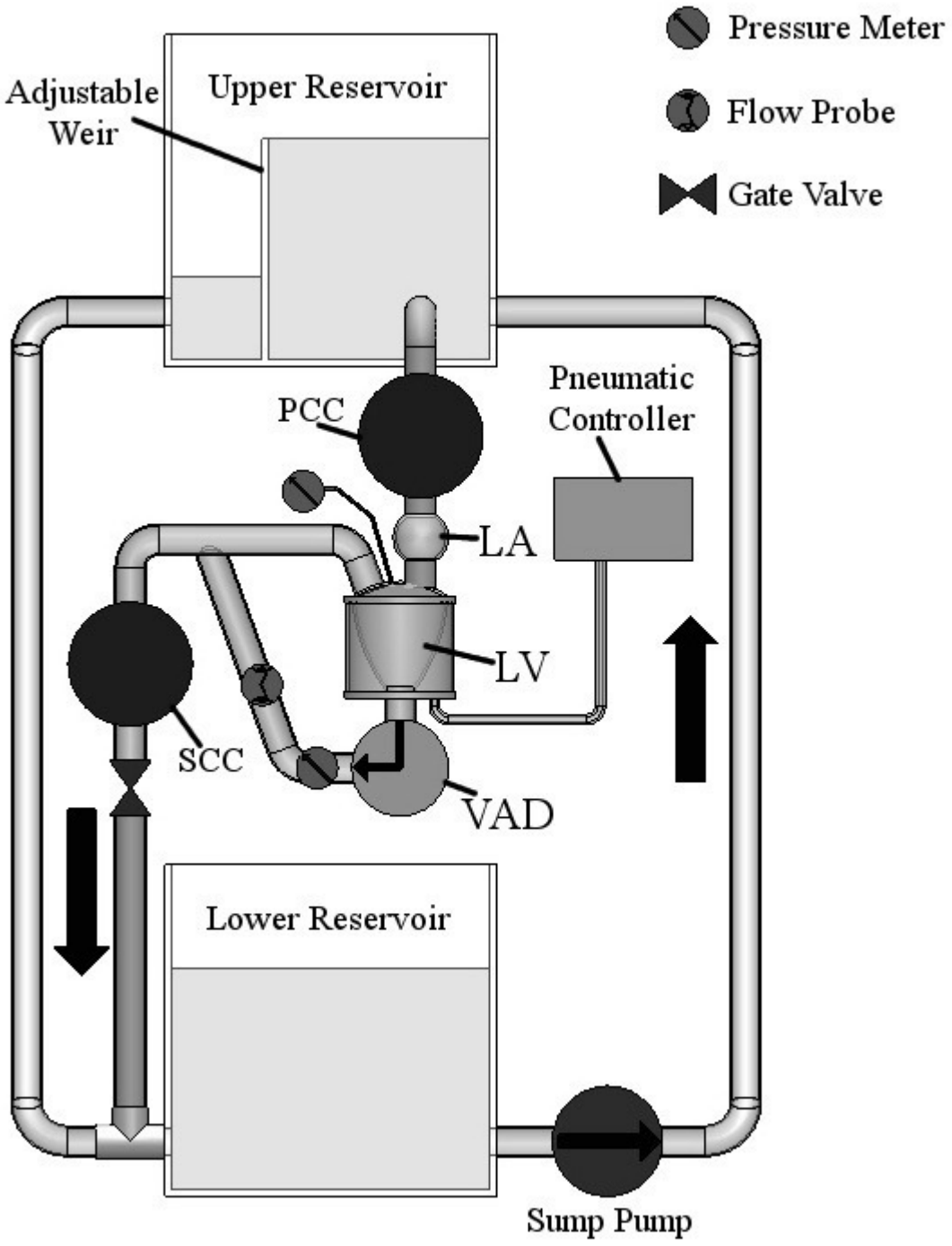


Figure 4.1. Schematic of mock circulation loop with pulsatile capability. PCC/SCC, pulmonary/systemic compliance chamber(s); LA, left atrium; LV, left ventricle. Not shown: unidirectional pericardial valves at "top" of LV to represent mitral and aortic valves.

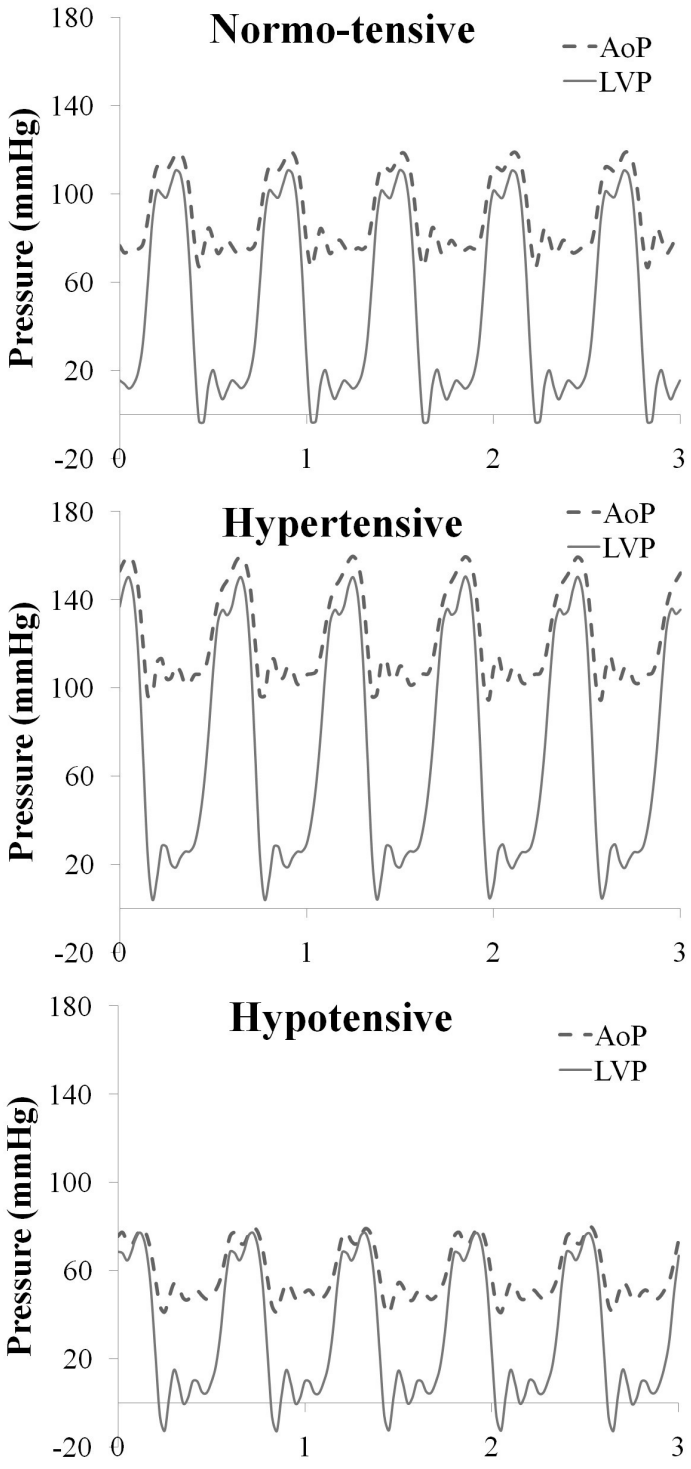


Figure 4.2. Oscillating pressure waveforms associated with each simulated cardiac condition: normo-tensive (a), hypertensive (b), and hypotensive (c). AoP, aortic pressure, LVP, left ventricular pressure [mmHg].

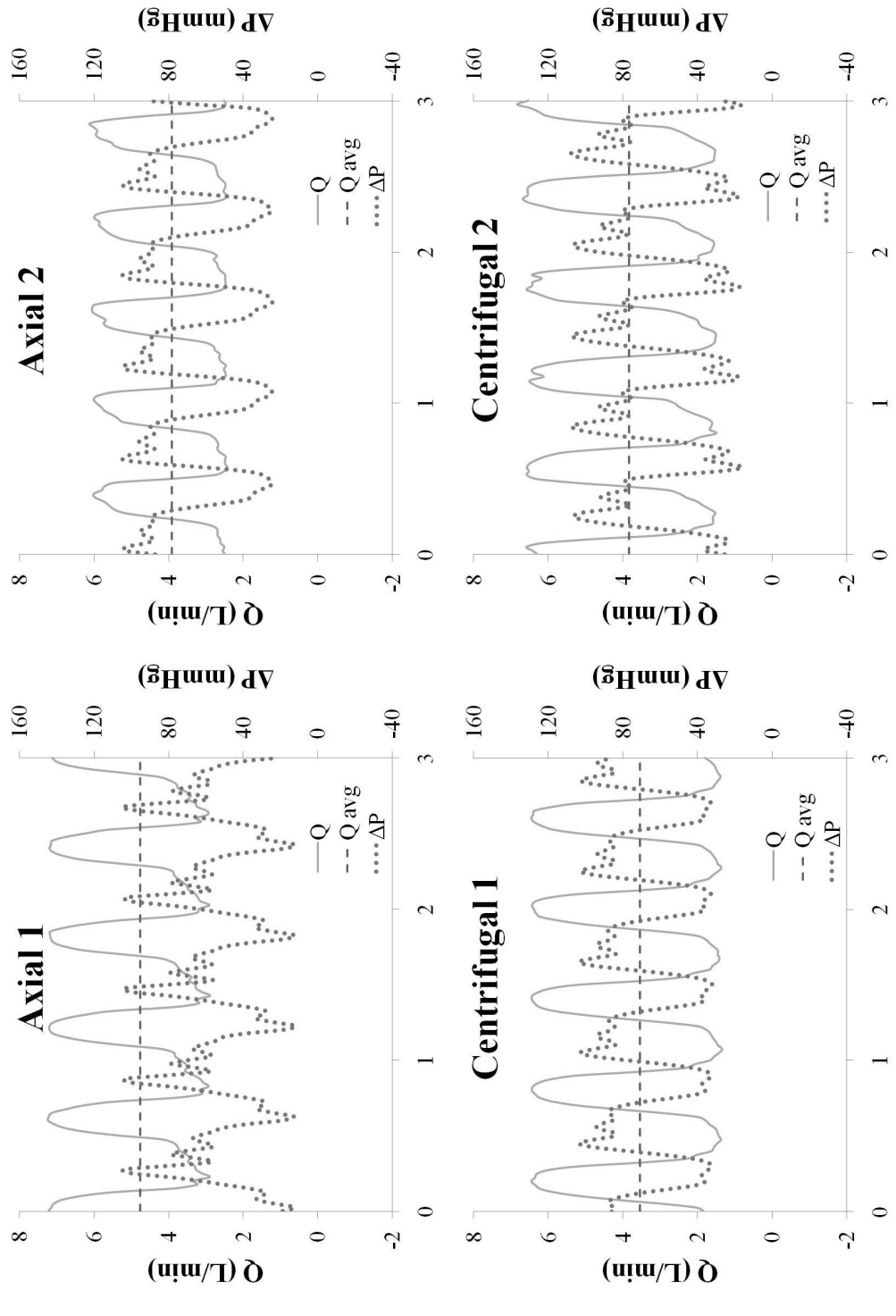


Figure 4.3. Oscillating pressure and flow waveforms under normo-tensive condition for axial (A1, A2) and centrifugal (C1, C2) continuous-flow pumps. Q, flow rate [L/min]; ΔP, pressure differential [mmHg].

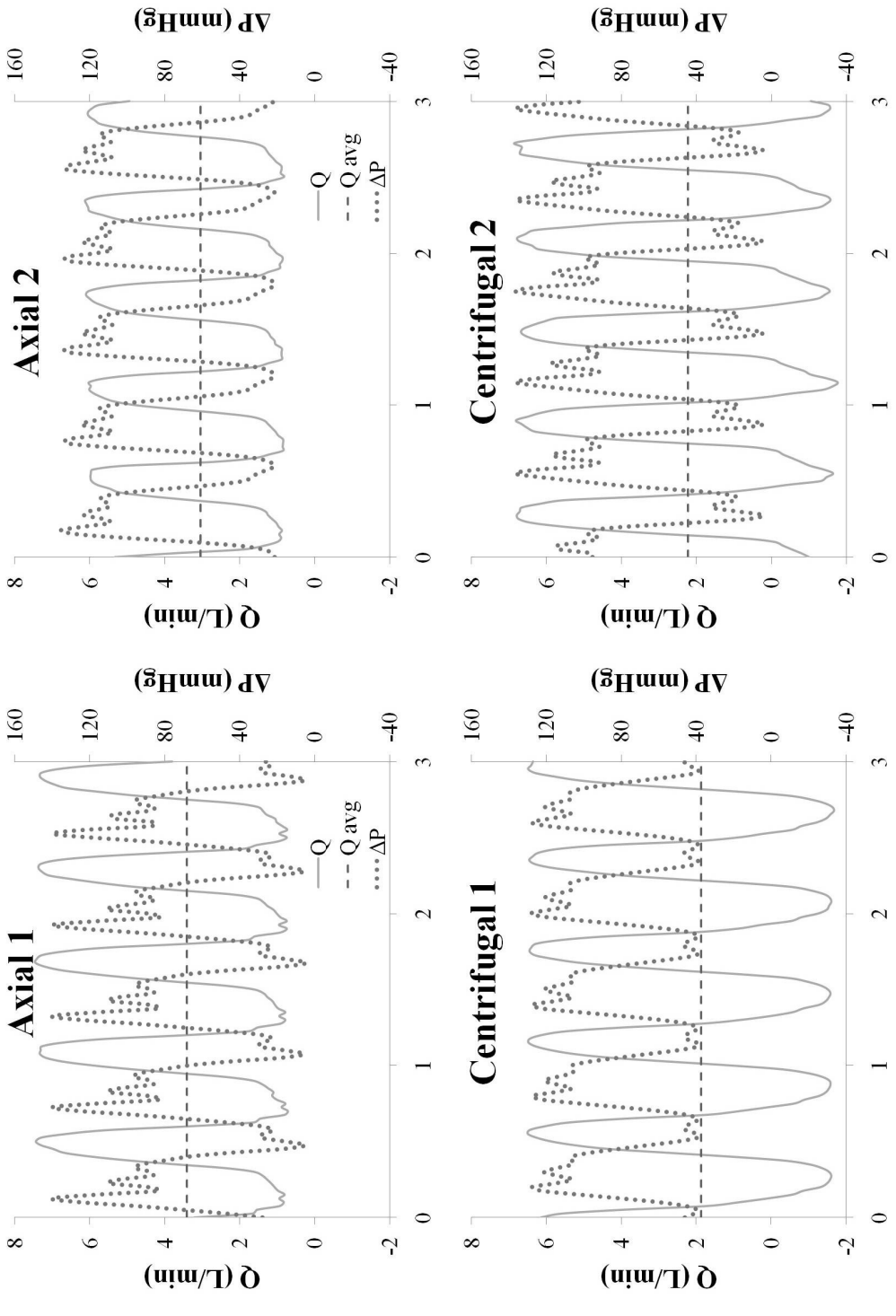


Figure 4.4. Oscillating pressure and flow waveforms under hypertensive condition for axial (A1, A2) and centrifugal (C1, C2) continuous-flow pumps. Q, flow rate [L/min]; ΔP, pressure differential [mmHg].

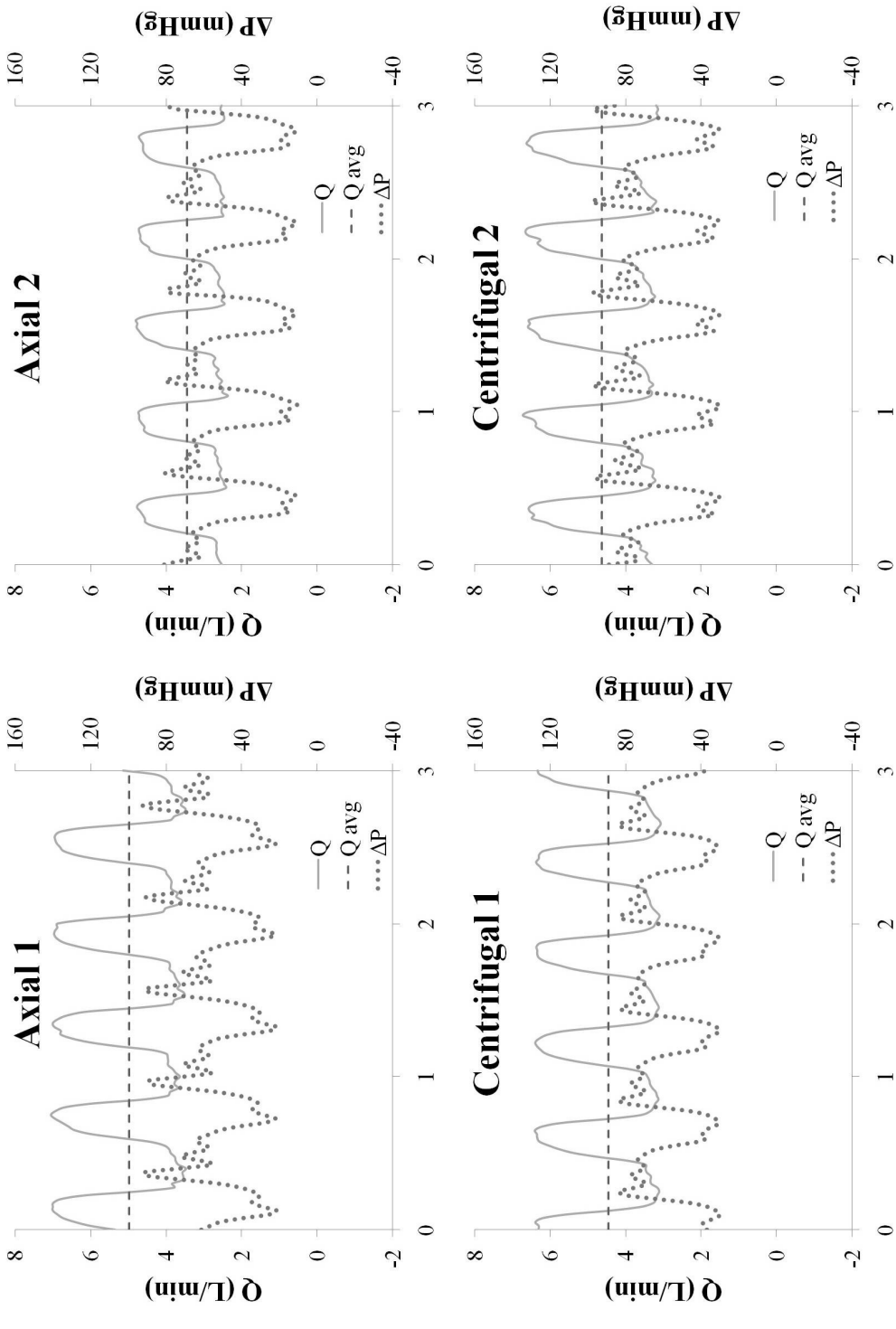


Figure 4.5. Oscillating pressure and flow waveforms under hypotensive condition for axial (A1, A2) and centrifugal (C1, C2) continuous-flow pumps. Q, flow rate [L/min]; ΔP, pressure differential [mmHg].

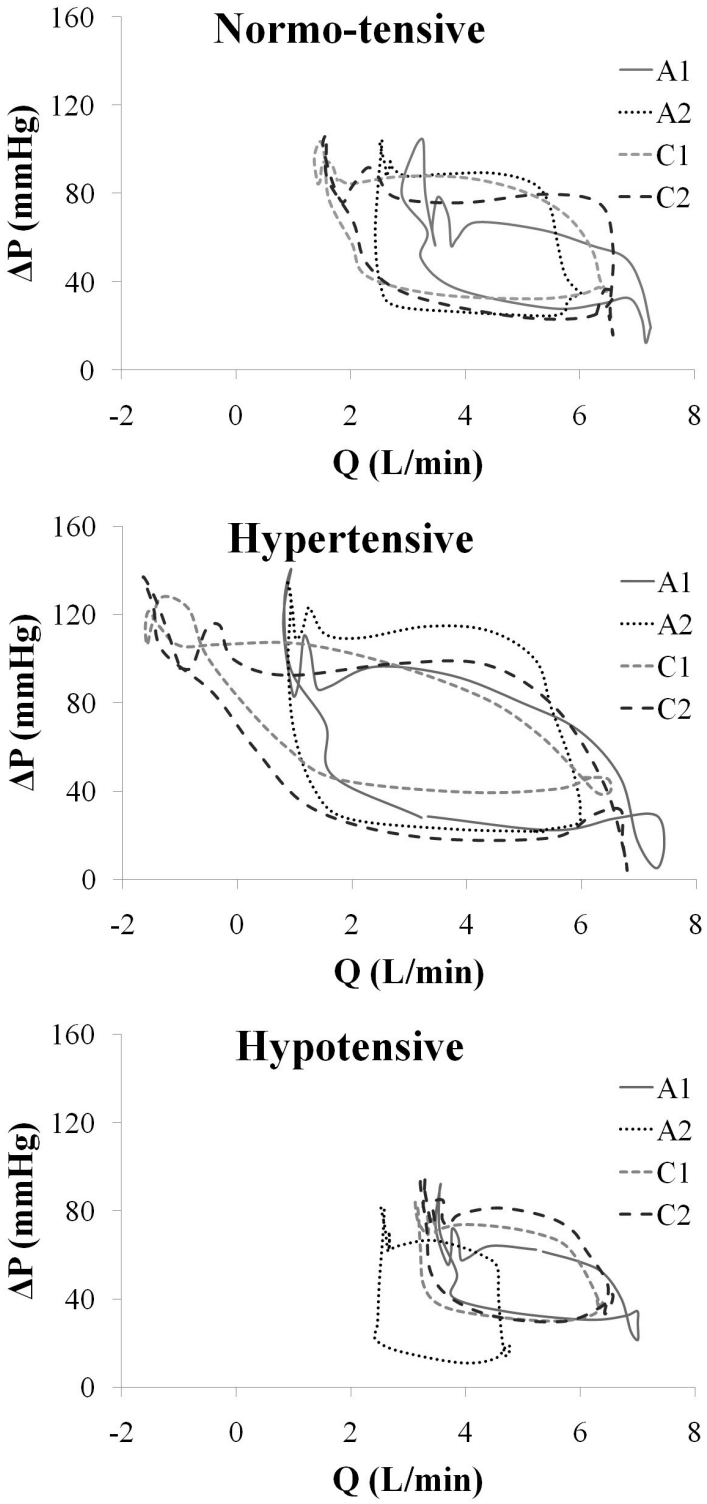


Figure 4.6. Pressure-flow (ΔP-Q) performance curves for all four devices under the three tested conditions. Q, flow rate [L/min]; ΔP, pressure differential [mmHg].

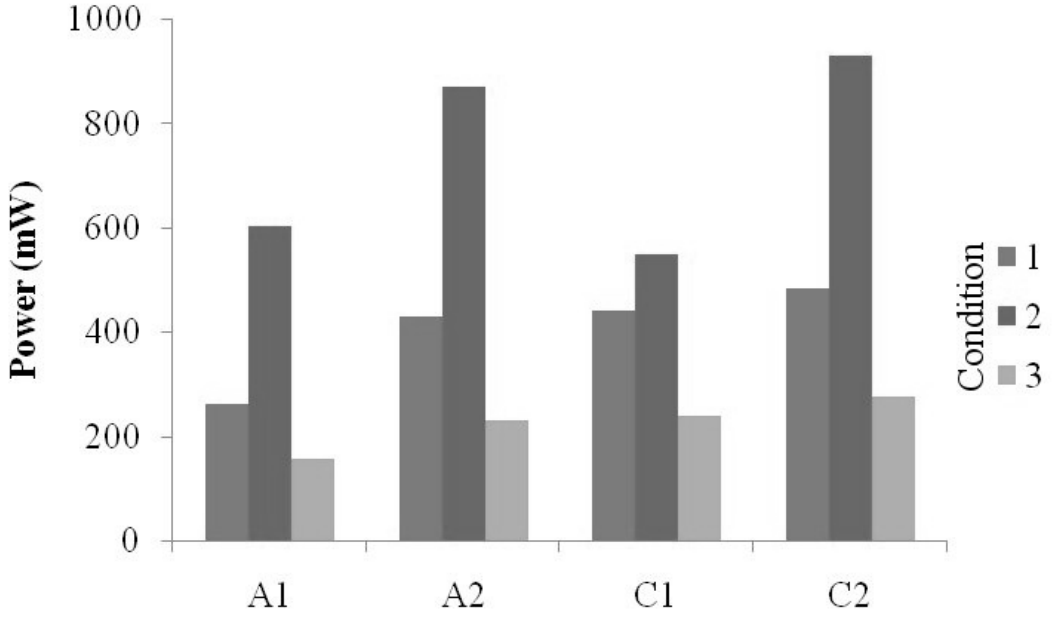


Figure 4.7. Hydraulic power supplied by each VAD in a typical cycle under the pulsatile cardiac models [mW].

Table 4.1. Cardiac conditions for pulsatile flow analysis. LVP, left ventricular pressure [mmHg]; LAP, left atrial pressure [mmHg]; MAP, mean arterial pressure [mmHg].

| **Condition** | **Model** | **LVP** | **LAP** | **MAP** |
|---|---|---|---|---|
| 1 | Normo-tensive | 110 | 15 | 90 |
| 2 | Hypertensive | 150 | 15 | 120 |
| 3 | Hypotensive | 80 | 5 | 60 |

Table 4.2. Flow rate, pressure differential, and pulsatility results for axial- and centrifugal-flow devices under the pulsatile cardiac models. Q, flow rate (L/min); ΔP, pressure differential (mmHg); $PI_Q$, flow pulsatility index; $R_{pul}$, pulsatility ratio. One-way ANOVA was used to Q and ΔP across both devices and conditions, with *p*-values for column data in the last two rows. *Indicates significant difference across row (single condition). †Indicates significant difference among column (single device).

| **Condition** | **Metric** | **Axial 1 (A1)** | **Axial 2 (A2)** | **Centrifugal 1 (C1)** | **Centrifugal 2 (C2)** |
|---|---|---|---|---|---|
| **Speed** | | **9000** | **10000** | **2000** | **2000** |
| 1 | Q ± SD | 4.8±1.6 | 3.9±1.4 | 3.5±2.0 | 3.8±2.0 |
| | ΔP ± SD | 55±24 | 66±28 | 68±24 | 64±29 |
| | $PI_Q$ | 0.96 | 1.00 | 1.49 | 1.51 |
| | $R_{pul}$ | 0.56 | 0.80 | 1.40 | 1.04 |
| 2 | Q ± SD | 3.4±2.5† | 3.1±2.1 | 1.9±3.1† | 2.2±3.2† |
| | ΔP ± SD | 70±38 | 81±40 | 82±32† | 73±41 |
| | $PI_Q$ | 2.01 | 1.79 | 4.41 | 4.01 |
| | $R_{pul}$ | 1.03 | 1.25 | 3.96 | 2.17 |
| 3 | Q ± SD ($p$<0.0004) | 5.0±1.3 | 3.4±0.9* | 4.5±1.3 | 4.6±1.3 |
| | ΔP ± SD ($p$<0.03) | 53±19 | 47±23*† | 59±18 | 63±21 |
| | $PI_Q$ | 0.74 | 0.72 | 0.76 | 0.80 |
| | $R_{pul}$ | 0.54 | 0.47 | 0.81 | 0.73 |
| ALL | Q | $p$<0.01 | $p$=0.20 | $p$=0.001 | $p$=0.002 |
| | ΔP | $p$<0.09 | $p$=0.001 | $p$<0.01 | $p$<0.50 |

# CHAPTER 5

# CONCLUSIONS AND FUTURE WORK

## 5.1 Conclusions

This dissertation has resulted in three original manuscripts submitted to various peer-reviewed journals for publication consideration. Further, an open-loop mock circulatory system has been developed, which is capable of independent preload and afterload regulation that is able to generate low to negative pressure differentials, in addition to high pressure differentials, across tested ventricular assist devices (VADs). In addition, three hypotheses were tested:

- Hypothesis 1 stated that centrifugal-flow VADs will have higher hydraulic efficiency over axial-flow. As shown in Chapter 2, the centrifugal-flow devices demonstrated greater capacity, fewer hydraulic losses, lower resistance, and thus, greater hydraulic efficiency when compared to the axial-flow devices.
- Hypothesis 2 stated that centrifugal-flow VADs will be more pressure sensitive over axial-flow. Based on the results and discussion in Chapter 3, the centrifugal-flow devices have similar pressure sensitivity to the axial-flow devices at higher flow rates (6-8 L/min), they have a significant difference in pressure sensitivity at intermediate to low flow rates, including those near standard physiological conditions.

- Hypothesis 3 stated that centrifugal-flow VADs will have greater pulsatility over axial-flow. As publicized in Chapter 4, both the axial- and centrifugal-flow devices are capable of maintaining some level of pulsatile flow when connected in parallel with a pulsating ventricle model. However, the centrifugal design exhibits significantly greater pulsatility index and pulsatility ratio under physiological conditions of varying preload and afterload.

Initially, the work was focused on flow characteristics under steady-state, continuous-flow conditions. In Chapter 3, the steady-state data was used to create a computational model of varying flow. The following chapter employed experimental methods to analyze, validate, and discuss device performance under an oscillating pressure and flow environment, analogous to the implanted configuration. All statistical analyses were carried out by means of *t*-test or one-way analysis of variance (ANOVA). Statistical significance was considered at $p < 0.05$.

In conclusion, the centrifugal-flow pumps show considerable hydraulic advantages under physiologic conditions. Further, the developed mock loop is capable of generating pressure differentials important to proper modeling of the physiological system, and to device performance characterization testing.

## 5.2 Limitations

Various caveats and limitations for each of the studies in this manuscript are reported within respective chapters. Here some global constraints are outlined pertaining to the entire work contained in this dissertation. First, only a single speed was employed for analysis of each device. Care was taken, both hydrodynamically and

clinically, to ensure that selected speeds would be employable for device comparison. Second, various metrics (pressure sensitivity, pulsatility index, pulsatility ratio, etc) may have an impact on biological or hematological compatibility. However, these tests were all carried out *in vitro* with a working fluid hydraulically similar to blood, but different otherwise.

Each flow loop used in the studies contained within this dissertation, while fulfilling the design intent, is by no means exact in modeling the physiologic circumstance. Further, the theoretical models for ventricular behavior are only speculative in nature. The models do mimic some natural occurrences, but are only used as a generic set of data to compare device performance.

Finally, as outlined in the first chapter, there are multiple "generations" used to classify VADs. The devices used here fall under both second and third generation devices. Both axial-flow devices employ a magnetic motor and mechanical (contacting) bearing within the blood flow path of the device, classifying them as second generation. The two centrifugal-flow pumps also have magnet-driven motors, but do not use mechanical bearings. Instead, the devices rely on magnetic levitation or a hydrodynamic bearing. Additionally, only one of each device has been tested. It is assumed that the device manufacturers apply a variability tolerance control limit on device performance. Thus, the performance noted in this work would be subject to some statistical window of variability, of which only a single point of reference is concluded here.

## 5.3 Suggestions for Future Work

The relevance of conclusions made herein should be further studied. A few suggestions for future work are outlined below.

- Multiple speeds: The data collected and presented herein could benefit by supplemental studies carried out in the same manner but using additional impeller speeds to monitor the impact of speed metrics such as pressure sensitivity and pulsatility index.
- Mulitple designs: This study employs two axial-flow and two centrifugal-flow blood pumps. Collecting similar data on other pump designs (axial-, centrifugal-, and mixed-flow) could yield further validation of the conclusions.
- Physiologic conditions: To gain insightful data on device performance, additional settings could be designed on the pulsatile-flow mock circulation loop to mimic other physiological conditions not modeled here.
- Ventricular unloading, etc (*in vitro*): It would be useful and clinically-relevant to study device performance for ventricular unloading, pump occlusion, adverse events, and other situations pertinent to the implantable configuration. For example, on the pulsatile-flow mock loop, the pressures and flows could be measured and compared under conditions such as: pump on (baseline), pump off (pump failure), pump on with aortic valve occluded (aortic stenosis), pump on with nonclosing aortic valve (aortic regurgitation), and pump on with inflow directed toward ventricle wall (ventricular suction).

Additional studies could be carried out in a more multidisciplinary approach. The following would be based on the availability of patient data and other resources necessary for *in vivo* experiments and data collection.

- Statistical design of study: *In vivo* data from multiple patients and statistical modeling (design of experiments, etc) capability coupled with clinician input could add knowledge to the scientific community regarding the application of axial- and centrifugal-flow device differences. This could be done for a number of metrics, including ventricular unloading, hemodynamics, end organ function, microcirculation, biocompatibility, and hemocompatibility.